POSTER PRESENTATION

Sciences/Agriculture/Environment and Technology

Graduate School

Valaya Alongkorn Rajabhat University under the Royal Patronage

HPLC ANALYSIS OF NUCLEOSIDES AND NUCLEOBASES FROM THE COMMERCIAL BY AVAILABLE PRODUCTS OF *CORDYCEPS*.

Khanittha Cordhanam[1], Uthai Sakee[2], Watchara Kanchanarach[3]

[1] Department of Chemistry, Faculty of Science, Mahasarakham University, e-mail; nidta_ning@hotmail.com

[2] Department of Chemistry, Faculty of Science, Mahasarakham University, e-mail; uthai.s@msu.ac.th

[3] Department of Biology, Faculty of Science, Mahasarakham University, e-mail; wkanchanarach@yahoo.com

ABSTRACT

Cordyceps is one of well-known traditional Chinese medicine (TCM), While purines and pyrimidines are thought to be its bioactive ingredients. Therefore, determination of these compounds is helpful to understand the origins of nucleosides in *Cordyceps*. A high performance liquid chromatography (HPLC) was developed for the determination of five purine and pyrimidine, namely uridine, inosine, guanosine, adenosine and cordycepin in the commercially available products of *Cordyceps*. The separation was performed on An ACE-5 C18-AR column (4.6 x 250 mm x 5 mm.) and gradient elution of methanol and 5 mM aqueous triethylamine, and UV detection at 254 nm. The correlation coefficients of five analytes were high ($R^2 > 0.995$) within test ranges. The overall R.S.D.s for intra-day and inter-day for five analytes were less than 3.57 and 4.57%, respectively. The developed of method was applied for analysis of nucleoside and nucleobases in the commercial available products of *Cordyceps*.

Keywords: *Cordyceps* ; High performance liquid chromatography; nucleosides; nucleobases; commercial available products of *Cordyceps*.

Introduction

Cordyceps, one of the most valued traditional Chinese medicines, consists of the dried fungus *Cordyceps* growing on the larva of caterpillar. It is also known as ‘‘summer-grass and winter worm’’ because of its appearance during different seasons. The parasitic complex of the fungus and the caterpillar is found in the soil of a prairie at an elevation of 3,500 to 5,000 meters. It is commonly used in China for over two thousand years. It is growing in popularity because of its attributed extraordinary health benefits like enhanced physical stamina for superior performance, anti-cancer and protection for lungs and kidneys, night sweating, hyperglycemia, hyperlipidemia, hyposexualities, asthenia after severe illness, respiratory disease, renal dysfunction and renal failure, arrhythmias and other heart disease, and liver disease (Zhu et al., 1998; Shao et al., 2003; Shashidhar et al., 2013).

Nucleosides are considered the main bioactive component in *Cordyceps* (Li et al., 2002), involved in the regulation and modulation of various physiological processes in body through purinergic or pyrimidine receptors (Ralevic et al.,1998;Jacobson et al., 2002), are recognized to be the main bioactive components in *Cordyceps* (Le et al., 2006). To date, more than 10 nucleosides and their related compounds, including adenine, adenosine, cytosine, cytidine, uridine, guanine, guanosine, hypoxanthine, inosine, thymine, thymidine, 2’-deoxyuridine and cordycepin have been isolated and identified from *Cordyceps*. (Le et al.,2006). Adenosine and cordycepin have been used as a marker for the quality control of *Cordyceps* in Chinese Pharmacopoeia (Ballarin et al., 1987). Adenosine and cordycepin were pharmaceutically active components exhibits multiple pharma-cological actions such as immunomodulatory (Kim,2010; Yu et al., 2007), pharmacokinetic effects (Tsai et al., 2010), cardioprotection, Anti-cancer

effects (Yoshikawa etal., 2011), antileukemic (Kodama et al., 2000), etc. Several techniques were available for the analysis of nucleosides in *Cordyceps* such as thin layer chromatography (TLC) (Ma et al., 2008), high performance liquid chromatography (HPLC) (Song et al., 2008) and capillary electrophoresis (Li et al.,2008). Ion-pairing reversed-phase liquid chromatography (IP-RP-LC-MS) has been commonly used in other fields for the separation of nucleosides (Yang et al., 2010). In this report, five main nucleosides namely uridine, inosine, guanosine, adenosine, and cordycepin in commercial available products of *Cordyceps* were simultaneously determined by HPLC.

Research Objectives

To developed method for determination of five analytes, namely uridine, inosine, guanosine, adenosine, and cordycepin in commercial available products of *Cordyceps* by high performance liquid chromatography (HPLC) with UV detector.

Methodology

Chemicals

Nucleobases such as uridine, inosine, guanosine were purchased from Acros (New Jersey, USA). Nucleoside such as adenosine was purchased from Acros (New Jersey, USA) and cordycepin was purchased from Sigma (St.Louis, MO, USA). HPLC grade methanol form Carol Erba Reagent SpA. Triethylamine form Carol Erba Reagent SpA, deionized water. A stock standard solution was prepared in methanol.

Samples

The commercial by available products of *Cordyceps* (11 samples) were purchased from difference market and online market located in Thailand. The samples were classified according *Cordyceps* species: 6 were made from pure *Cordyceps militaris* and 5 samples were made from *Cordyceps sinensis* and other of ingredients.

Preparation of standard solution and calibration curve

The commercial by available products of *Cordyceps* 0.5 g were ground and then mix with 25 mL of methanol aqueous solution and then ultrasonic extraction was performed at room temperature for 30 min repeat for 3 times. After filtration, the solution was evaporated. The crude extraction was dissolved with methanol and inject into HPLC condition.

HPLC analysis

Analysis was performed on Shimadzu LC-20AC liquid, a chromatograph, equipped with diode array detection (DAD) system. An ACE-5 C18-AR column (4.6 x 250 mm x 5 mm.) and an ACE-5 C18-AR guard column (4.6 x 12.5 mm x 5 mm.) were used. Solvents that constituted the mobile phase were used A (5 mmol/L aqueous TEA) and B (methanol). The separation was achieved using gradient elution on 0-25% B for 30 min. The injection volume was used 20 µL. The flow rate was 1 mL/min. The analytes were monitored at 254 nm. (Fan et at., 2006, 2007; Yang et al., 2008; Gao et al., 2007)

Research Results

Method validation

The linearity, regression and linear ranges of five analytes were performed using the developed HPLC method. The linearity of each standard was confirmed by plotting the peak area ratio and the concentration of standard. The high correlation coefficient (R^2 > 0.995) values indicated good correlations between investigated compounds concentrations and peak area ratios. The limits of detection and quantification were lower than 0.145 ng/mL and 14.643 ng/mL, respectively as show in Table 1.

Table 1. Linear regression data, limit of detection (LOD), limit of quantification (LOQ) and % recovery of the investigated compounds.

Analytes	Linear regression			LOD (ng/mL)	LOQ (ng/mL)	%Recovery
	Linear range (µg/mL)	Regression equation	R^2			
U	1.75-100.00	y = 3787x + 13083	0.999	2.059	6.863	109.09
I	0.25-80.00	y = 2404x - 10394	0.995	4.393	14.643	107.57
G	0.70-50.00	y = 3146x + 3905	0.995	2.977	9.925	102.20
A	0.25-175.50	y = 8058x + 35442	0.998	1.385	4.617	102.49
C	0.50-200.00	y = 25300x +36574	0.999	0.145	0.482	94.74

U; Uridine, I; Inosine, G; Guanosine, A; Adenosine, C; Cordycepin

R^2, squares of correlation coefficients for the standard curves

LOD, limit of detection = 3 × SD/Slope

LOQ, limit of quantification = 10 × SD/Slope

%Recovery = 100 × (amount found – original amount)/amount spike

Intra-day and inter-day variations were chosen to determine the precision of the method. For intra-day variability test, the standard solutions were analyzed in triplicates for three times within 1 day, while for inter-day variability test, the samples were examined in triplicate for consecutive 3 days. The repeatability present as the relative standard deviation for intra-day and inter-day variations of less than 3.57 and 4.57%, respectively as show in Table 2. Recovery was performed by adding known amounts of five investigated components into a certain amount (0.05 g) of the commercial by available products of *Cordyceps*. The recoveries of uridine, inosine, guanosine, adenosine and cordycepin were 109.09, 107.57, 102.20, 102.49 and 94.74%, respectively.

Table 2. Intra-day and inter-day variability for the assay of the investigated compounds.

Analytes	intra-day		inter-day	
	%Accuracy	%R.S.D	%Accuracy	%R.S.D
Uridine	100.36	1.71	93.23	2.10
Inosine	98.25	0.76	99.55	3.53
Guanosine	99.06	3.57	100.75	1.53
Adenosine	100.04	2.82	93.73	4.57
Cordycepin	99.17	3.42	100.38	2.39

Mean and relative standard deviation (R.S.D.s) for three replicates.

R.S.D. (%) = 100×S.D./mean.

Quantitative determination of purine and pyrimidine in commercial *cordyceps*

Chromatograms of the commercial by available products of *Cordyceps* were shown in Fig. 1. The investigated compounds were identified by comparison of their

retention times with those obtained on injecting standards under the same conditions or by spiking *Cordyceps* samples with stock standard solutions.

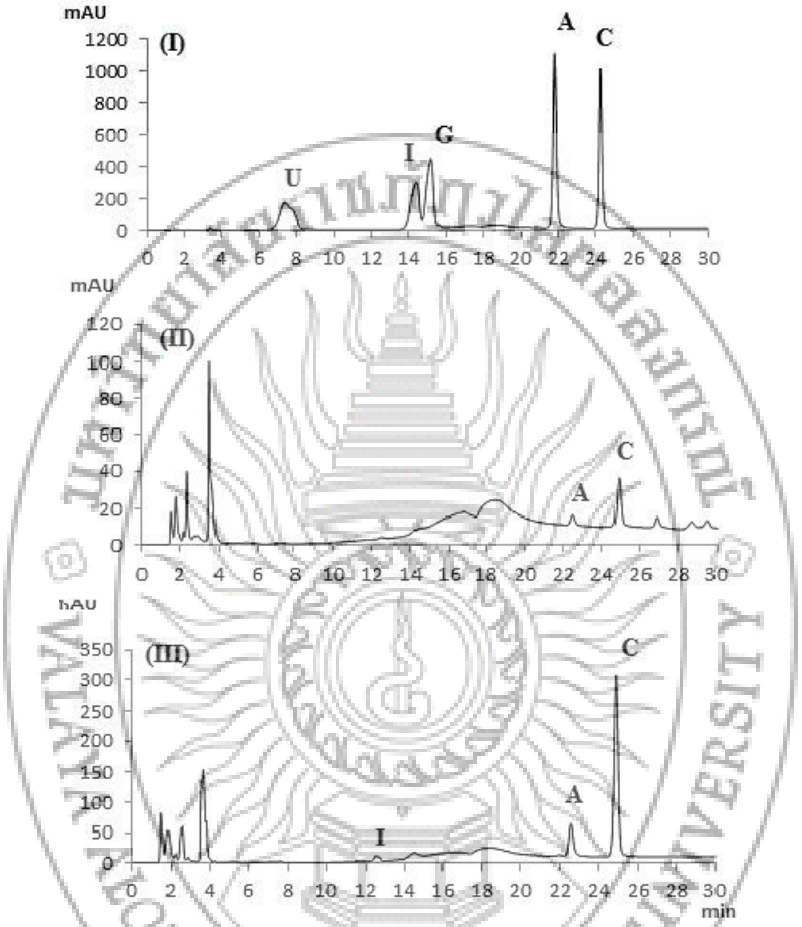

Fig. 1. HPLC profiles of (I) mixed standards, (II) the commercial by available products of *Cordyceps*; No.9 and (III) the commercial by available products of *Cordyceps*; No.10. U; Uridine, I; Inosine, G; Guanosine, A; Adenosine, C; Cordycepin

Contents of five analytes in the commercial by available products of *Cordyceps* are summarized in Table 3. In this study, the commercial by available products of *Cordyceps* were divided into two part, the extracted from *Cordyceps militaris* (No.1,2,3,7,10 and 11) and *Cordyceps sinensis* (No.4,5,6,8 and 9). The contents of

adenosine and cordycepin in samples were higher than other investigated compound. In commercial by available products of *Cordyceps militaris*, the contents of adenosine and cordycepin were higher than those in samples from *Cordyceps sinensis*, which is similar to another previous report. (Yu et al.,2006). In the commercial by available products of *Cordyceps* the contents of analytes were 1.70-434.86 mg/g (adenosine) and 5.21-411.65 mg/g (cordycepin), only No.10 were 11.82 mg/g (uridine) and 48.94 mg/g (inosine). It means that the contents of adenosine and cordycepin were important for commercial product.

Table 3. The contents (mg/g) of five investigated compound in the commercial by available products of *Cordyceps*

Number	Uridine	Inosine	Gianosine	Adenosine	Cordycepin
1.	-	-	-	362.47±0.90	349.04±0.34
2.	-	-	-	-	188.76±0.20
3.	-	-	-	1.70±0.10	109.95±0.30
4.	-	-	-	-	5.21±0.16
5.	-	-	-	132.73±0.63	-
6.	-	-	-	-	-
7.	-	-	-	76.82±1.04	167.03±0.63
8.	-	-	-	18.53±0.41	39.71±0.22
9.	-	-	-	9.85±0.43	31.33±0.24
10.	11.82±0.92	48.94±0.25	-	434.86±0.91	411.65±0.37
11.	-	-	-	34.93±0.47	176.56±0.11

The all values are reported as the mean ± standard deviation (n = 3). Mean values with different letters are significantly different ($p < 0.05$)

Summary and Recommendation

In this study, a simple and convenient high performance liquid chromatography (HPLC) methods for determination of nucleosides and nucleobases namely uridine, inosine, guanosine, adenosine and cordycepin. The proposed method might be useful for quality control and authentication of *Cordyceps* samples. Within the content profiles

of nucleosides and nucleobase in *Cordyceps* product, adenosine and cordycepin were confirmed as a marker for the commercial by available products of *Cordyceps*. Simultaneous determination of five analytes in the commercial by available products of *Cordyceps* was performed, which provides a sample and sensitive method with good linearity, precision and recovery. The method was applied for the analysis of nucleosides and nucleobases in the commercial by available products of *Cordyceps*.

Acknowledgement

This work was supported by Mahasarakham University, Human Resource Development in Science Project (Science Achievement Scholarship of Thailand; SAST), the Center of Excellence for Innovation in Chemistry (PERCH-CIC) and the Division of Research Facilitation and Dissemination, Mahasarakham University

References

Ballarin, M.,Herrera-Marschitz, M.,Casas,M.,&Ungerstedt, U.(1987). Striatal adenosine levels measured 'in vivo' by micro dialysis in rats with unilateral dopamine denervation. **Neuroscience Letter**. 3, 338–344.

Fan H, Li S.P., Xiang J.J., Lai C.M., Yang F.Q., Gao J.L., Wang Y.T. (2006). Qualitative and quantitative determination of nucleosides, bases and their analogues in natural and cultured *Cordyceps* by pressurized liquid extraction and high performance liquid chromatography–electrospray ionization tandem mass spectrometry (HPLC–ESI-MS/MS). **Anal. Chem Acta**. 567, 218–228.

Fan H, Yang F.Q, Li S.P. (2007). Determination of purine and pyrimidine bases in natural and cultured *Cordyceps* using optimum acid hydrolysis followed by high performance liquid chromatography. **Journal of Pharmaceutical and Biomedical Analysis**. 45, 141–144

Gao J.L., Kelvin S.Y. Leung , Y.T. Wang , C.M. Lai , S.P. Li , L.F. Hu , G.H. Lu, Z.H. Jiang , Z.L. Yu.(2007). Qualitative and quantitative analyses of nucleosides and nucleobases in *Ganoderma* spp. by HPLC–DAD-MS. **Journal of Pharmaceutical and Biomedical Analysis**. 44, 807–811.

Jacobson K.A., Jarvis M.F., Williams M. (2002). Purine and pyrimidine (P2) receptors as drung targets. **J. Med. Chem**, 45, 4057–4093.

Kim, S. D. (2010). Isolation, structure and cholesterol esteraseinhibitory activity of a polysaccharide, PS-A, from *Cordyceps sinensis*. **Journal of the Korean Society for Applied Biological Chemistry**, 53, 784–789.

Kodama, E. N., Mc Caffrey, R. P., Yusa, K., & Mitsuya, H. (2000). Antileukemic activity and mechanism of action of cordycepin against terminal deoxynucleotidyl transferase-positive (TdT^+) leukemic cells. **Biochemical Pharmacology**, 59, 273–281.

Li S. P., Yang, F. Q., & Tsim, K. W. K. (2006). Quality control of *Cordyceps sinensis*, a valued traditional Chinese medicine. **Journal of Pharmaceutical and Biomedical Analysis**, 41, 1571–1584.

Li, J.,Feng,C.,Ni,X.,&Zhang,W.(2008). Determination of nucleosides of natural *Cordyceps sinensis* in Qinghai province by capillary electrophoresis. **Journal of Chinese Pharmaceutical Sciences**. 43 , 1105–1107.

Li, S., Su, Z., Dong, T.,& Tsim, K. (2002).The fruiting body and its caterpillar host of *Cordyceps sinensis* show close resemblance in main constituents and anti-oxidation activity . **Phytomedicine**. 9,319–324.

Ma, Y.,Wang,Y.(2008). Determination of nucleosides in *Cordyceps sinensis* preparation by dual-wavelength TLC scanning. **China Pharmacy**. 20, 2375–2377.

Ralevic V., Burnstock G. (1998). Receptors for purines and pyrimidines. **Pharmacol. Rev**. 50,413–492.

Shao P. Li, Kui J. Zhao, Zhao N. Ji, Zong H. Song, Tina T.X. Dong, Chun K. Lo, Jerry K.H. Cheung, Shang Q. Zhu, Karl W.K. Tsim. (2003). A polysaccharide isolated from *Cordyceps sinensis*, a traditional Chinese medicine, protects PC12 cells against hydrogen peroxide-induced injury. **Life Sciences**. 73, 2503–2513.

Shashidhar. M.G., Giridharc P., Udaya Sankar K., Manohar B. (2013). Bioactive principles from *Cordyceps sinensis*: A potent food supplement–A review. **Journal of function food**. 5, 1013-1030.

Song, J., Liu, C., Li, D., Jin, B.(2008). Determi nation of cordycepin from cultured *Cordyceps sinensis* by HPLC-DAD. **Food Science**. 40 , 352–354.

Tsai, Y., Lin, L., & Tsai, T. (2010). Pharmacokinetics of adenosine and cordycepin, a bio-active constituent of *Cordyceps sinensis* in rat. **Journal of Agricultural and Food Chemistry**. 58, 4638–4643.

Yang F.Q., Li S.P.(2008). Effects of sample preparation methods on the quantification of nucleosides in natural and cultured *Cordyceps*. **Journal of Pharmaceutical and Biomedical Analysis**. 48, 231–235.

Yang,F.,Li,D.,Feng,K.,Hu,D.,Li,S.(2010). Determination of nucleotides, nucleosides and their transformation products in *Cordyceps* by ion-pairing reversed-phase liquid chromatography–mass spectrometry. **J of Chromatography A**. 34. 5501–5510.

Yoshikawa, N., Nishiuchi, A., Kubo, E., Yamaguchi, Y., Kunitomo, M., Kagota, S., Shinozuka, K., & Nakamura, K. (2011). *Cordyceps sinensis* acts as an adenosine A3 receptor agonist on mouse melanoma and lung carcinoma cells, and human fibrosarcoma and colon carcinoma cells. **Pharmacology & Pharmacy**. 2, 266–270.

Yu L.M, Zhao J, Li S.P, Fan H, Hong M, Wang Y.T, Zhu Q. (2006)0 Quality evaluation of *Cordyceps* through simultaneous determination of eleven nucleosides and bases by RP-HPLC. **J. Sep. Sci**. 29, 953–958.

Yu, L., Zhao, J., Zhu, Q., & Li, S. (2007). Macrophage biospecific extraction and high performance liquid chromatography for hypothesis of immunological active components in *Cordyceps sinensis*. **Journal of Pharmaceutical and Biomedical Analysis**. 44, 439–443.

Zhu, J.S., Halpern, G.M., Jones, K. (1998). The scientific rediscovery of an ancient Chinese herbal medicine: *Cordyceps sinensis*: Part I. **Journal of Alternative and Complementary Medicine**. 4, 289–303.

DEVELOPING OF A PRIMER SET IN *SRY* GENE FOR DNA DETECTION BY LOOP-MEDIATED ISOTHERMAL AMPLIFICATION (LAMP) METHOD FROM HUMAN BLOOD, SEMEN AND SALIVA SAMPLES

Anupong Sukjai[1], Monthira Monthatong[2] and Khemika Lomthaisong[3]

[1]Department of Biology, Faculty of Science, Khon Kaen University, Khon Kaen, 40002, Thailand; Email: sanupongia@gmail.com
[2]Department of Biology, Faculty of Science, Khon Kaen University, Khon Kaen, 40002, Thailand; Email: monmon@kku.ac.th
[3]Forensic Science Program, Faculty of Science, Khon Kaen University, Khon Kaen, 40002, Thailand; Email: khemlo@kku.ac.th

ABSTRACT

Loop mediated isothermal amplification (LAMP) is a highly effective specific and sensitive technique used for amplification of specific DNA region under isothermal conditions without thermal cycler requirement, as well as simple and low cost method. The LAMP products can be detected by agarose gel electrophoresis and also by visual turbidity. The objective of this research is to develop primers which specific to *SRY* gene in LAMP assay. A set of four LAMP primers were designed using PrimerExplorer V4 software based on the human *SRY* gene (accession number: NM_003140.2) obtained from the GenBank database. Designed primers were further tested in LAMP reaction. The amplification reaction was performed at 67 ºC for 60 min. The results revealed that the set of developed primers in the present study could detected all male DNA from human blood, semen and saliva samples by LAMP method. The amplified products can be visualized both by gel electrophoresis and visual detection. Therefore, designed LAMP primers in this research are an alternatively valuable tool of sex determination for biological evidence in forensic caseworks.

Keywords: Loop mediated isothermal amplification, *SRY* gene, Sex determination, Blood sample, Semen sample, Saliva sample

Introduction

Molecular biological tool revolutionized forensic investigation is *the analysis of DNA*. As all organisms contain DNA exhibiting variability among individuals, any biological materials associated with a legal case carries in information about their sources (Jobling & Gill, 2004). Forensic DNA analysis plays an important role in the criminal justice community aiding conviction of the guilty and exoneration of the innocent. Remained tissues or cells from missing persons and victims of mass disasters have been re-associated and identified through linking reference samples to recovered remains (Butler, 2015).

Because the analysis of DNA is the key to the conviction or exoneration of suspects and the identification of victims of crimes, accidents and disasters, the innovative techniques in molecular biology are conducted to analyze DNA which obtained from biological samples or evidences. For example, polymerase chain reaction or PCR, was developed in the 1980s by Kary Mullis and colleagues. PCR is a scientific technique in molecular biology to amplify a single or a few copies of the DNA fragment in a PCR tube, generating thousands to millions of copies of a particular DNA sequence (Valones

et al., 2009). However, PCR technique requires sophisticated equipment and spends much time detecting for the amplified products in the molecular laboratory facilities. Therefore, the associated cost is also high. Loop mediated isothermal amplification (LAMP) was developed to solve problems of PCR method which was first described by Tsugunori Notomi and co-workers in 2000. LAMP is a highly effective specific and sensitive technique used for DNA amplification, amplifies target DNA from a few copies to 10^9 copies under an isothermal temperature of 60-65 °C in less than 1 hour without thermal cycler requirement, as well as simple and low cost method. Considering the benefits of rapid amplification, simple process and easy detection, LAMP is a valuable tool for the diagnosis in developing countries without requiring sophisticated equipment, small laboratory or fieldwork (Parida, Sannarangaiah, Dash, Rao, & Morita, 2008). LAMP has become increasingly popular for assay of a wide range of samples. For medical diagnosis, there is a lot of research that uses LAMP technique to detect diseases such as tuberculosis (Iwamoto, Sonobe, & Hayashi, 2003), dengue virus (Parida et al., 2005), HIV (Curtis, Rudolph, & Owen, 2008) and parasite (Fallahi, Mazar, Ghasemian, & Haghighi, 2015). In forensic science, LAMP is still using less than other molecular approach. Thus, LAMP should be conducted and applied to forensic evidence. It could be manipulated DNA evidence, which is most often used in sexual assault cases and murder cases (Prottas & Noble, 2007).

Sex determination can be crucial in forensic casework such as murder rape cases or cases of missing persons (Wurmb-Schwark, Bosinski, & Ritz-Timme, 2007). In forensic casework, determining the gender of the source of forensic DNA evidence is routinely performed by PCR of a region of the *sex-determining region Y* (*SRY*) located only on Y chromosomes short arm region 1 band 1 sub band 3 range from bases 2,654,895 to 2,655,781 which is the master regulator of male sex determination. Under appropriate PCR condition, no PCR amplicon is produced with female while the amplicon presents with male DNA of *SRY* gene (Drobnic, 2006; Kastelic, Budowle, & Drobnic, 2009; Tozzo et al., 2013). DNA sample sources for detection or DNA analysis obtain from nucleated cells that are present in biological materials left at crime scenes such as blood semen bone teeth tissues hairs urine and saliva (Butler, 2012).

Objective

The aim of this research was to develop primers which specific to *sex-determining region Y* (*SRY*) gene in LAMP technique. In addition, amplification of specific human *SRY* gene region by using LAMP for human DNA detection and sex determination from human blood, semen and saliva samples which were usually found on crime scene will be examined.

Materials and methods

1. Human blood, semen and saliva samples

Blood samples (n=5) were kindly provided from Blood Bank Srinagarind hospital, Khon Kaen University. Semen samples (n=5) were obtained from andrology laboratory Srinagarind hospital, Khon Kaen University. Saliva samples (n=5) were collected from unrelated volunteers. All specimens were transferred to laboratory in ice box to preserve the live cells. They were immediately extracted as soon as we obtained. Moreover, female blood and female saliva were also prepared and used as a negative control for LAMP specificity testing since *SRY* gene cannot be found in female. Prior to sample

collection and DNA analysis, the Khon Kaen University Ethics committee in Human Research had granted ethical approval for the study (HE581415).

2. DNA extraction

In order to obtain the best DNA quality and yield, 50 µL each of specimens was extracted by using GF-1 Blood DNA Extraction Kit (Vivantis, Malaysia) for blood samples, Illustra tissue & cells genomicPrep Mini Spin Kit (GE Healthcare, USA) for semen and saliva samples following to the manufacturer's protocol. The extracted DNA will be further used in LAMP assay.

3. LAMP assay

3.1 Primer design

To design the LAMP primers, the human *SRY* gene (accession number: NM_003140.2) obtained from the GenBank database. The set of primers was designed manually in accordance with the standard parameters of the PrimerExplorer V4 software (https://primerexplorer.jp/e/) to recognize a total of six distinct regions of the *SRY* gene. Moreover, each primer was tested for similarities with other sequences available in the GenBank databases using the BlastN algorithm (https://blast.ncbi.nlm.nih.gov/ Blast.cgi).

3.2 LAMP reaction

The LAMP reaction was carried out in a total volume 25 µL containing 2.5 µL 10× Isothermal Amplification Buffer (New England Biolabs, USA, including 20 mM Tris-HCl (pH 8.8), 10 mM $(NH4)_2SO_4$, 50 mM KCl, 2 mM $MgSO_4$, 0.1% Tween® 20), 1.6 µM each FIP and BIP, 0.2 µM each F3 and B3, 1.4 mM dNTPs (Vivantis, Malaysia), 0.8 M Betaine (Sigma-Aldrich, Canada), 6 mM $MgSO_4$, 8.0 U *Bst* 2.0 DNA polymerase (New England Biolabs, USA) and 2 µL DNA obtained in a way that we described above. To improve the specificity, the mixture was incubated at 67 ºC for 60 min, followed by heating at 80 ºC for 5 min to inactivate the enzyme and terminate the reaction. The LAMP products were visualized by (1) gel electrophoresis using a 2% agarose gel stained with ethidium bromide and (2) visual turbidity under natural light by comparison between positive samples and negative control.

3.3 LAMP specificity testing

The specificity of the designed primers was performed by using DNA extracted from female blood and female saliva as template. Furthermore, sex determination was also examined here.

Results

1. LAMP primers

In this study, four primers for LAMP, including two outer primers (F3 and B3) and two inner primers (FIP and BIP) were designed to recognize a total of six distinct regions of the *SRY* gene. The designed primers and primers positions on *SRY* gene are shown in Table 1 and Figure 1.

2. Detection of human *SRY* gene by LAMP reactions

The human *SRY* gene in the DNA samples of 5 male bloods, 5 semen and 5 male saliva was amplified. Reaction tubes were visually examined after completion of the amplification and propriety of DNA amplification was confirmed by the presence of white turbidity which observed by naked eye under natural light (Figure 2). Moreover, amplification product with a ladder pattern was confirmed by 2% agarose gel and

stained with ethidium bromide (Figure 3, 4 and 5). The results of the detection of human *SRY* gene are summarized in Table 2.

3. LAMP specificity

The specificity of the LAMP reaction for *SRY* gene detection was evaluated by reactions with DNA obtained from female blood and female saliva. Clear laddering pattern was observed only for *SRY* gene from male DNA. LAMP reactions with other DNA did not show any positive results, confirming the specificity of the LAMP reaction for *SRY* detection (Figure 3, 4 and 5).

Table 1 *SRY* specific primer set for LAMP reaction.

Primer	Type	Position on gene	Length	Sequence (5'-3')'
F3	Forward outer	464-482	19mer	TCTTCCAGGAG GCACAGAA
B3	Backward outer	633-652	20mer	TGGCTTTCGTAC AGTCATCC
FIP (Forward inner primers)	F1c (Forward inner)	523-543	21mer	CGCCTTCCGAC GAGGTCGATA
	F2 (Forward inner)	483-502	20mer	ATTACAGGCCA TGCACAGAG
BIP (Backward inner primers)	B1c (Backward inner)	557-578	22mer	AGAATTGCAGT TTGCTTCCCGC
	B2 (Backward inner)	609-628	20mer	ACAACCTGTTG TCCAGTTGC

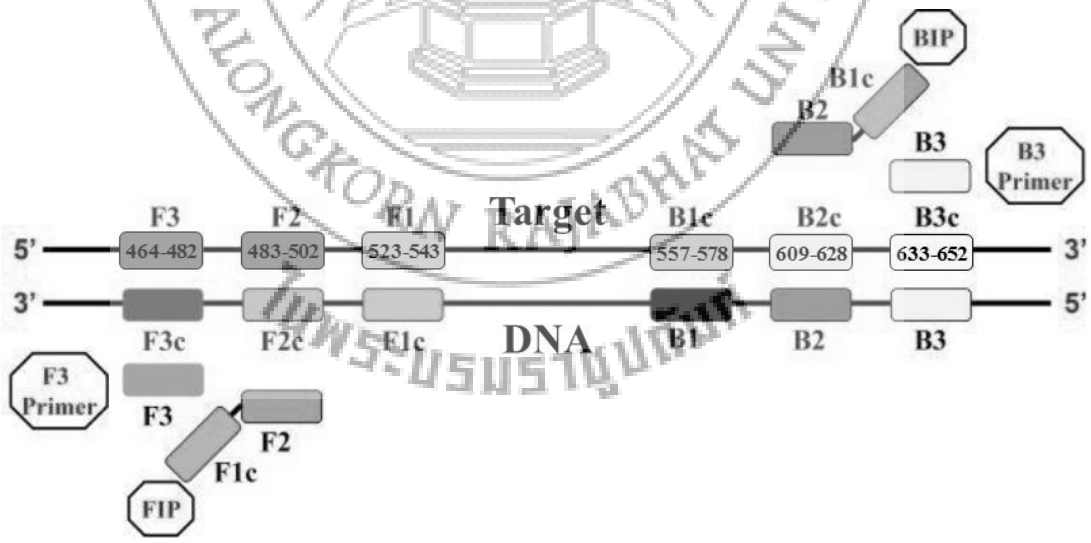

Figure 1. Positions of designed LAMP primers on target DNA.

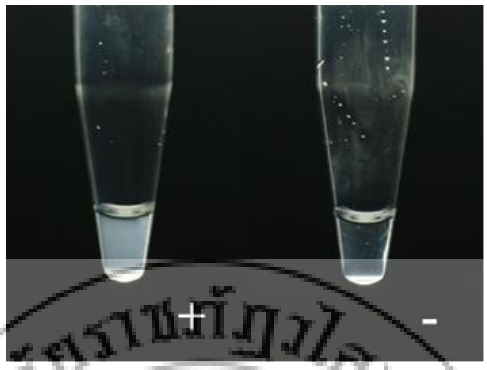

Figure 2. Detection of LAMP amplified products by visual examination. Positive LAMP reaction (+), negative control (-).

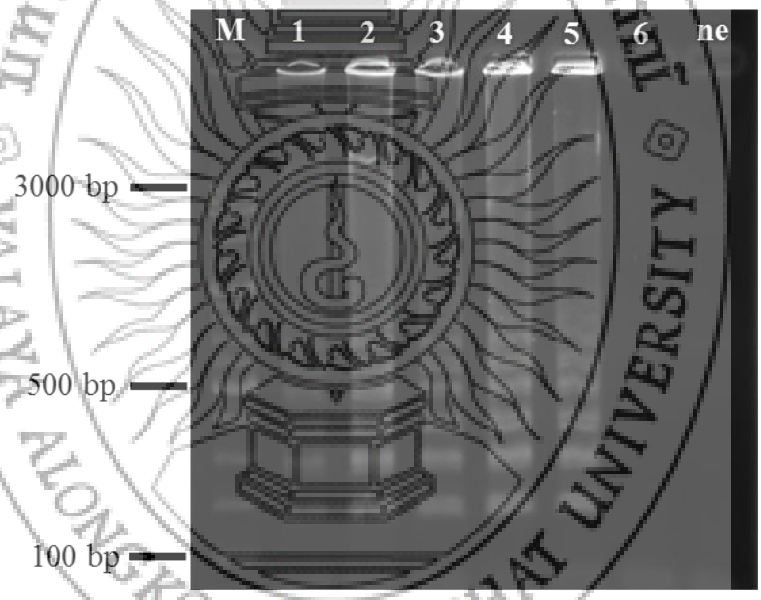

Figure 3. Confirmation of LAMP amplified products by 2% agarose gel electrophoresis stained with ethidium bromide. Lane M: 100 bp DNA marker, lane 1-5: male-blood samples, lane 6: female blood, lane ne: negative control (water).

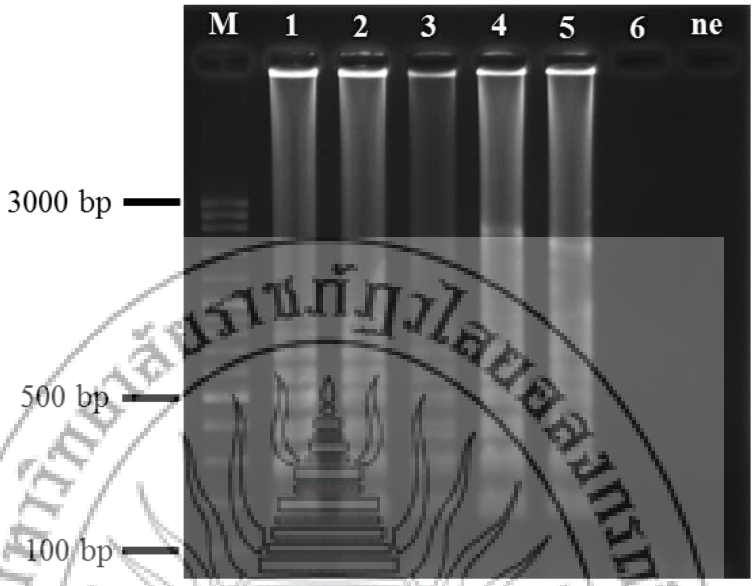

Figure 4. Confirmation of LAMP amplified products by 2% agarose gel electrophoresis stained with ethidium bromide. Lane M: 100 bp DNA marker, lane 1-5: semen samples, lane 6: female blood, lane ne: negative control (water).

Figure 5. Confirmation of LAMP amplified products by 2% agarose gel electrophoresis stained with ethidium bromide. Lane M: 100 bp DNA marker, lane 1-5: male-saliva samples, lane 6: female saliva, lane ne: negative control (water).

Table 2 Number of samples show the detection of human *SRY* gene

Samples	LAMP results	
	Positive to Turbidity	**Positive to Gel electrophoresis**
Blood (n=5)	5	5
Semen (n=5)	5	5
Saliva (n=5)	5	5

Discussion and conclusion

We investigated a new developed primers for sex determination in LAMP assay by using human *SRY* gene. One of the advantages of LAMP assay is its efficacy to amplify specific sequences of target DNA under isothermal conditions (Nagamine, Hase, & Notomi, 2002; Notomi et al., 2000). Most importantly, this assay does not require a denatured DNA template (Nagamine, Watanabe, Ohtsuka, Hase, & Notomi, 2001; Nagamine et al., 2002). The auto-cycling strand displacement DNA synthesis is achieved by DNA polymerase with high strand displacement activity within the rage of 60-65 ºC. In this study, we performed amplification temperature at 67 ºC to optimize the reaction for improving specificity (Tanner & Evans, 2014).

The results show that all male DNA from blood, semen and saliva samples revealed positive results to LAMP method. Moreover, female DNA from female blood and female saliva gave negative results. LAMP technique has been demonstrated to be specific in that it employs four primers recognizing a total of six distinct regions of the *SRY* gene. Thus, for amplification to occur, all primers must anneal to their complementary region. It indicated that developed LAMP primers in this research can amplify the human *SRY* gene using the LAMP assay with high efficiency, specificity and rapidity. This method makes it possible to easily determine the gender without thermal cycling or electrophoresis which requires just 60 min to accomplish. Therefore, we concluded that LAMP can alternatively be used for sex determination from human blood samples, semen and saliva.

Moreover, sex determination by LAMP method with designed primer set specific to *SRY* gene should prove its value in various application for forensic investigations, such as unknown bodies of mass disasters, sexual assaults cases. In addition, it might be useful in screening prenatal diagnosis of fetus with a known family history of genetic disorder affecting only male children.

Acknowledgement

This research was supported by Science Achievement Scholarship of Thailand (SAST).

References

Butler, J. M. (2012). **Advanced Topics in Forensic DNA Typing: Methodology.** Massachusetts: Academic Press.

Butler, J. M. (2015). The future of forensic DNA analysis. **Philosophical Transactions of the Royal Society B**. 370, 1-10.

Curtis, K. A., Rudolph, D. L., & Owen, S. M. (2008). Rapid detection of HIV-1 by reverse-transcription, loop-mediated isothermal amplification (RT-LAMP). **Journal of Virological Methods**. 151, 264–270.

Drobnic, K. (2006). A new primer set in a *SRY* gene for sex identification. ***International Congress Series***. 1288, 268–270.

Fallahi, S., Mazar, Z. A., Ghasemian, M., & Haghighi, A. (2015). Challenging loop-mediated isothermal amplification (LAMP) technique for molecular detection of **Toxoplasma gondii. Asian Pacific Journal of Tropical Medicine**. 8(5), 366-372.

Iwamoto, T., Sonobe, T., & Hayashi, K. (2003). Loop-mediated isothermal amplification for direct detection of *Mycobacterium tuberculosis* complex, *M. avium*, and *M. intracellulare* in sputum samples. **Journal of Clinical Microbiology.** 41(6), 2616–2622.

Jobling, M. A., & Gill, P. (2004). Encoded evidence: DNA in forensic analysis. ***Nature Reviews Genetics.*** 5, 739-751.

Kastelic, V., Budowle, B., & Drobnic, K. (2009). Validation of *SRY* marker for forensic casework analysis. **Journal of Forensic Sciences**. 54(3), 551-555.

Nagamine, K., Watanabe, K., Ohtsuka, K. Hase, T., & Notomi, T. (2001). Loop-mediated isothermal amplification reaction using a nondenatured template. **Clinical Chemistry**. 47(9), 1742-1743.

Nagamine, K., Hase, T., & Notomi, T. (2002). Accelerated reaction by loop-mediated isothermal amplification using loop primers. ***Molecular and Cellular Probes.*** 16, 223-229.

Notomi, T., Okayama, H., Masubuchi, H., Yonekawa, T., Watanabe, K., Amino, N., & Hase, T. (2000). Loop-mediated isothermal amplification of DNA. **Nucleic Acids Research**. 28(12), e63.

Parida, M., Horioke, K., Ishida, H., Dash, P. K., Saxena, P., Jana, A. M., … Morita, K. (2005). Rapid detection and differentiation of dengue virus serotypes by a real-time reverse transcription–loop-mediated isothermal amplification assay. **Journal of Clinical Microbiology**. 43(6), 2895-2903.

Parida, M., Sannarangaiah, S., Dash, P. K., Rao, P. V. L., & Morita, K. (2008). Loop mediated isothermal amplification (LAMP): a new generation of innovative gene amplification technique; perspectives in clinical diagnosis of infectious diseases. ***Reviews in Medical Virology***. 18, 407-421.

Prottas, J. M., & Noble, A. A. (2007). Use of forensic DNA evidence in prosecutors' offices. **Journal of Law, Medicine & Ethics**. 35(2), 310-315.

Tanner, N. A., & Evans, T. C., Jr. (2014). Loop-Mediated Isothermal Amplification for Detection of Nucleic Acids. **Current Protocols in Molecular Biology**. 105, 15.14.1–15.14.14.

Tozzo, P., Giuliodori, A., Corato, S., Ponzano, E., Rodriguez, D., & Caenazzo, L. (2013). Deletion of *amelogenin* Y-locus in forensics: literature revision and description of a novel method for sex confirmation. **Journal of Forensic and Legal Medicine**. 20, 387-391.

Valones, M. A. A., Guimaraes, R. L., Brandao, A. A. C., Eleuterio de Souza, P. R., Carvalho, A. A. T., & Crovela, S. (2009). Principles and applications of polymerase chain reaction in medical diagnostic fields: a review. ***Brazilian Journal of Microbiology.*** 40, 1-11.

Wurmb-Schwark, N. V., Bosinski, H., & Ritz-Timme, S. (2007). What do the X and Y chromosomes tell us about sex and gender in forensic case analysis? **Journal of Forensic and Legal Medicine**. 14, 27-30.

DROUGHT RELATED GENE EXPRESSION IN KDML105 RICE INDUCED BY *TRICHODERMA HARZIANUM* UNDER DROUGHT STRESS

Namphueng Moolphuerk[1] and Monthira Monthatong[1]
[1]Department of Biology, Faculty of Science, Khon Kaen University, Khon Kaen 40002, Thailand
Namphuengsc@hotmail.com

ABSTRACT

The study aims to investigate drought responsive gene expressions which are *NPR1, P5CS* and *SPS1* in KDML105 rice treating with *T. harzianum* under drought stress. The germinated seeds were cultivated in 2 experiments including *T. harzianum*-treated soil through treating with 3×10^7 spores/ml and untreated soil experiment until seedlings were twenty-one days old. Then, *T. harzianum*-treated soil experiment was divided into 2 groups which are *T. hazianum*-treated group (C+*Th*) and *T. hazianum*-treated group (D+*Th*) as well as untreated soil experiment was divided into 2 groups including *T. hazianum*-untreated group (C) and *T. hazianum*-untreated group (D). Both D+*Th* and D groups were exposed to drought stress through withholding water for 5 days. The expression of *NPR1*, *P5CS* and *SPS1* was completely performed through quantitative real time RT-PCR (qRT-PCR). The *Protein Kinase* was also used as internal control. The results exhibited that the expression of *NPR1* was slightly up regulated in *T. harzianum*-treated rice with and without drought stress comparing to control plants. By contrast, the same gene was dramatically down regulated in untreated plants under drought stress. The *P5CS* expression was significantly increased in C+*Th* and D+*Th* groups comparing to untreated groups. As well, the expression of *SPS1* was significantly increased in C+*Th* and D+*Th* groups whereas the same gene expression was slightly decreased in D group comparing to control rice. As above results, we suggest that *T. harzianum* can alleviate drought stress through drought related gene induction.

Keywords: Drought, *Trichoderma*, gene expression, KDML105 rice

Introduction

In the recent year, water scarcity becomes an important problem in many areas worldwide. In Thailand, water shortage has directly affected to agriculture and economy because Thailand is one of important exporters in the world market exporting both processed and unprocessed agricultural products. Therefore, the rice and other crop yields continuously decrease. Thai Rice Exporters Association (2016) reported that in the year 2015, rice yield was decreased approximately 13.3 million tons compared with the previous year. Many areas in Thailand were also affected, especially in the Northeastern the main cultivated areas of Khao Dawk Mali 105 rice (KDML 105), an important crop as the staple food for world population, especially Asians. The effect of water scarcity leads to soil water content decreasing and disrupts plant growth and development causing declination of crop quantity and quality (Ministry of Natural Resources and Environment, 2014) (In Thai). The attemption of improving and developing drought tolerant plant and nonchemical agent is one of interesting alternative methods. The genus *Trichoderma*, a filamentous fungi free living in soils, erected by Persoon in 1794 but captured the attention of agriculturists after Weindling

and his associates (1932) exhibited that one species of the genus can inhibit other fungi and control plant diseases. Then, Shoemaker and coworker (1983) revealed that this genus can produce enzyme using in industry. Recently, several studies reported that *Trichoderma* can promote plant growth and also able to alleviate both biotic and abiotic stresses in various plants. The study of Bae and associates (2009) revealed that *T. hamatum DIS 219b* colonization induced the drought-altered expression of seven responsive drought ESTs in *Theobroma cacao* leaves. Nawrocka and Małolepsza (2013) reported that *Trichoderma* elicitors were involved in induction of defense mechanisms both induced systemic resistance (ISR) and systemic acquired resistance (SAR) leading to alteration on physiological, biochemical and molecular levels. Therefore, the present study purposes to investigate the expression of *T. harzianum*-induced gene which is *NPR1* gene encoding to Non-Expressor of *PR1* (*Pathogenesis Related*) protein. This protein acts as an important transcriptional co-activator of SA-responsive *PR* genes in SAR responding to abiotic and biotic stresses, moreover NPR1 protein has been involved in JA/ET-dependent defense responses in ISR responding to non-pathogen infection (Salas-Marina et al., 2011; Wu et al., 2012). Moreover, we also investigated drought tolerant related genes involving to compatible solute accumulation, an important drought responsive mechanism, which are *P5CS* and *SPS1*. The *P5CS* gene encodes to Δ'-pyrroline-5-carboxylate synthetase, a key enzyme in proline biosynthesis, (Hayat et al., 2012.) and *SPS1* gene encodes to sucrose phosphate synthase (SPS), the key enzyme in sucrose biosynthesis, (Okamura et al., 2011).

Objective

The present study purposes to investigate the expressions of *Trichoderma* induced gene which is *Non-Expressor of PR1* (*Pathogenesis Related1*) gene (*NPR1*) including drought tolerant related genes which are *P5CS* and *SPS1* in KDML105 rice seedlings under drought stress.

Materials and methods

Trichoderma preparation

T. hazianum was obtained from Department of Plant Pathogen, Faculty of Agriculture Kasetsart University, Kamphaeng Saen Campus, Nakhon Pathom, Thailand. For producing fresh culture, they were cultured on cooked rice seed and incubated at room temperature for seven days. Dose of *T. hazianum* was used as 3×10^7 spores/ml.

Rice plant growing

Rice seeds (*O. sativa* L.) cv. KDML105 obtaining from Khon Kaen Rice Research Center were surface sterilized with 80% ethanol for 30 seconds followed by 3% sodium hypochlorite solution with tween-20 then rinsed with steriled distilled water for three. Sterilized seeds were germinated on petri dish with Whatman filter paper saturating with sterile distilled water for five days.

Trichoderma inoculation

The equally germinated seeds were continuously cultivated dividing into 2 experiments. First, *T. harzianum*-treated experiment through soil treating with 100 ml/1 kg soil of 3×10^7 spores/ml and another is untreated experiment. Rice

seedlings were grown until twenty-one days old. Then, *T. harzianum*-treated experiment was divided into 2 groups which are *T. hazianum*-treated group (C+*Th*) and *T. hazianum*-treated group (D+*Th*) as well as untreated soil experiment was divided into 2 groups including *T. hazianum*-untreated group (C) and *T. hazianum*-untreated group (D). Both D+*Th* and D groups were exposed to drought stress through withholding water for 5 days, whereas C+*Th* and C groups were well watered. After 5 days of withholding water, leaf samples were harvested.

Rice leaf RNA extraction

About three hundred milligram of leaf samples were ground to fine powder in liquid nitrogen with a pre-chilled mortar and pestle. Then total RNA was extracted by using Vivantis® Nucleic acid extraction kit and performing follows manufacturer. Powdered leaf was transferred to 1.5 ml micro tube and 400 µl of Buffer TR were then added following centrifuge at 14,000 rpm for 3 minutes. Lysates were transferred into homogenization column following by centrifuge at 14,000 rpm for 2 minutes. The flow-through was saved and 350 µl of 80% ethanol were added to the flow-through. Six hundred and fifty microliter of sample were transferred into RNA binding column, then centrifuged at 10,000 rpm for a minute. The flow-through discarded and 500 µl of Wash Buffer were added with centrifuge at 14,000 rpm for 1 minute. The flow-through discarded and 70 µl of DNase I digestion mix were added into RNA binding column and incubated at room temperature for 15 minutes. Five hundred of Inhibitor Removal Buffer were then added following by centrifuge at 14,000 rpm for a minute. The flow-through was discarded and 500 µl of Wash Buffer were added. The RNA binding column was centrifuged at 10,000 rpm for a minute. The column was placed into a new 1.5 ml micro tube and 40 µl of RNase-free water was added onto membrane incubating for a minute. Finally, they were centrifuged at 10,000 rpm for a minute and stored at -80 °C.

The complementary DNA (cDNA) synthesis

The cDNA synthesis was performed by using the 2-step RT-PCR kit (Vivantis®) following manufacturer. The RNA-primer mixture comprising 0.5 µl of RNA template, 1 µl of 40µM oligo d(T)18, 1 µl of 10mM dNTPs mix and 7.5 µl of Nuclease-free water was prepared in a 0.2 ml micro centrifuge tube then the mixtures were incubated at 65 °C for 5 minutes and chilled on ice for 2 minutes. After 2 minutes, the mixtures were briefly spun down and added 10 µl of the cDNA synthesis mix comprising 2 µl of 10X Buffer M-MuLV, 0.5 µl of M-MuLV Reverse Transcriptase and 7.5 µl of Nuclease-free water into each RNA-primer mixture. Then, the mixtures were incubated at 42 °C for 60 minutes, following by incubating at 85 °C for 5 minutes. The cDNA was stored at -20 °C.

Drought tolerant-related gene expression

Drought tolerant-related gene expressions including *OsNPR1*, *OsP5CS* and *OsSPS1* genes were performed through quantitative real time RT-PCR (qRT-PCR). The drought tolerant-related gene specific primers were designed with Primer3 software version 0.4.0 (Table 1). The qRT-PCR mixtures were

prepared in 96 multiwell plate (Table 2) using Roache® Diagnostics, Thailand and the qRT-PCR reaction of each gene was completely conducted under appropriate condition (Table 3) using the LightCycler® 480. The result of gene expression analysis was presented as the relative expression comparing with the *protein kinase* (*PK*) gene using as internal control. The change of relative expression was calculated following the $2^{-\Delta\Delta Cp}$ method (Livak and Schmittgen, 2001). This method describes the change in expression of the target gene relative to some reference group such as control group.

$$\text{Fold change} = 2^{-\Delta\Delta Cp}$$

$\Delta\Delta C_p$: $(C_{p\ (\text{target gene})}-C_{p\ (\text{reference gene})})_{\text{treatment}}-(C_{p\ (\text{target gene})}-C_{p\ (\text{reference gene})})_{\text{control}}$

C_p: The C_p values provided from real-time PCR instrumentation

Table 1. The specific primers using in the study of drought tolerant-related gene

Primer	Sequences (5'→3')
1. NPR1 (F)	TCTCTTCCCTGTGCTTGCTT
NPR1 (R)	GACCATCTCCCCTCTCCTTC
2. P5CS (F)	CCACCAAGTGAACCATCATC
P5CS (R)	CGCTATTTGAAGCCAAGACA
3. SPS1 (F)	TCGCTGCTCTTCTTTCTGGT
SPS1 (R)	TGAGTCCATCTCCTCCTTCG
4. PK (F)	TCCTCTTTGGGTTTGGGTTT
PK (R)	CTTGCTCCTCTTGTCCCTGA

Table 2. The components of the qRT-PCR mixtures for the drought tolerant-related gene expression assay

Component	Amount/volume
1. cDNA template (diluted 1:5)	3 µl
2. Forward primer (10 µM)	0.2 µl
3. Reverse primer (10 µM)	0.2 µl
4. 2xLightCycler® 480 SYBR Green I Master	10 µl
5. Water	2.6 µl
Final volume	16 µl

Table 3. The appropriated condition of qRT-PCR for each drought tolerant related gene

Gene	Step	Temperature	Time	Cycle

		(°C)		
NPR1, *SPS1* and *PK*	Pre-incubation	95	10 minutes	1
	Amplification	95 60 72	10 seconds 10 seconds 20 seconds	45
	Melting curve	95 65 97	5 seconds 1 minute continuous	1
	Cooling	40	30 seconds	1
P5CS and *PK*	Pre-incubation	95	10 minutes	1
	Amplification	95 57 72	10 seconds 10 seconds 20 seconds	45
	Melting curve	95 65 97	5 seconds 1 minute continuous	1
	Cooling	40	30 seconds	1

Results

The effect of *T. harzianum* on drought tolerant gene expression including *NPR1*, *P5CS and SPS1* genes was completely examined using real-time quantitative PCR. The relative of gene expression was also analyzed using the $2^{-\Delta\Delta Cp}$ method (Livak and Schmittgen, 2001) and *Protein kinase* (*PK*) gene was used as reference gene or internal control. The results represented that *NPR1* expression was down regulated in drought treatments comparing with control. Whereas, *T. harzianum*-treated plants under drought stress and non-stress condition were slightly up regulated comparing to control plants. (Table 4, Figure 1A). Effect of *T. harzianum* on *P5CS* expression was then investigated. The results showed that *T. harzianum*-treated plants under non-stress condition were higher *P5CS* expression level than untreated-plants under same condition. Similarly, the *P5CS* expression level of *T. harzianum*-treated plants under drought stress was higher than untreated-plants significantly (Table 4, Figure 1B). The relative expression of *SPS1* was significantly increased (Table 4, Figure 1C) in *T. harzianum*-treated plants with and without drought stresses. While, the *SPS1* relative expression under drought stress was slightly decreased in untreated plants comparing to control.

Table 4. Effect of *T. harzianum* on drought tolerant-related gene expression including *NPR1*, *P5CS* and *SPS1* genes. Data are mean of the fold change ± SD (n = 3). Different letters indicate significant differences ($p<0.05$). 0.21

Treatment	***NPR1***	***P5CS***	***SPS1***
Control	1.00±0.00a	1.00±0.00a	1.00±0.00a
Control+*T. harzianum*	1.70±0.57a	2.70±0.16b	2.36±0.05b
Drought	0.08±0.58b	1.51±0.55a	0.89±0.09a
Drought+*T.harzianum*	1.14±0.64a	2.08±0.16c	1.68±0.45b

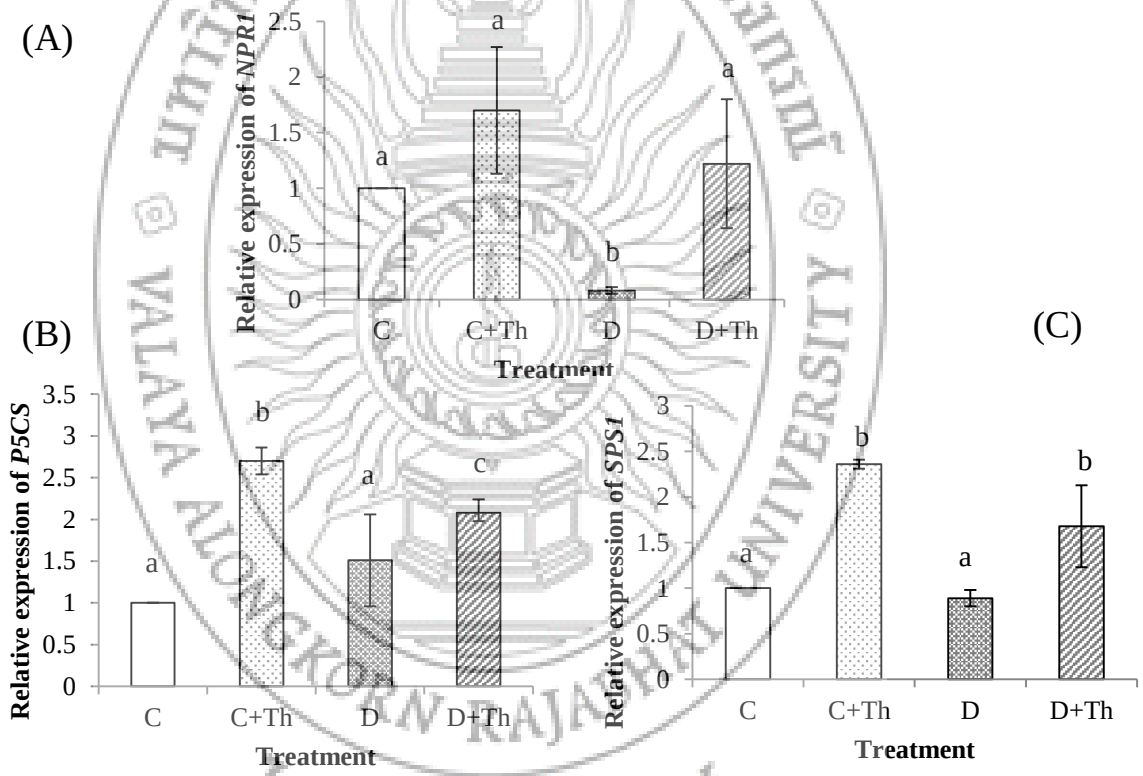

Figure 1. Effect of *T. harzianum* on drought tolerant-related gene expression including *NPR1* (A), *P5CS* (B) and *SPS1* (C) genes

Discussion and conclusion

Our study investigated effect of *T. harzianum* and drought stress on the expression pattern of *T. harzianum*-induced gene which is *NPR1* including drought tolerant related genes which are *P5CS* and *SPS1*. The *NPR1* gene encodes to Non-Expressor of *PR1* (*Pathogenesis Related*) protein acting as an important transcriptional

co-activator of SA-responsive *PR* genes in SAR responding to abiotic and biotic stresses, moreover NPR1 protein has been involved in JA/ET-dependent defense responses in ISR responding to non-pathogen infection (Salas-Marina et al., 2011; Wu et al., 2012). Our result showed that *NPR1* expression in *T. harzianum* colonized plants was slightly activated under drought and normal conditions when compared to uncolonized plants. Whereas, the same gene expression was down regulated dramatically in uncolonized plants under drought stress condition. Similarly, the study of Bassett et al. (2014) indicated that *NPR1* gene expression was suppressed in leaves of drought-exposed apple trees. The investigation involving the effect of *Trichoderma* spp. on *NPR1* expression under drought stress have been scarcely found. The most study focused on the effect of them to induce pathogen infected responsive system. Accordingly, the study of Salas-Marina et al. (2011) investigated that *T. atroviride* induced *PR-1a* and *PR-2* expression involving in SAR, plant defense system to plant pathogens, and also induced *PDF1.2* (*Plant-Defensin 1.2*) and *LOX-1* (*Lipoxygenase 1*) involving in ISR under foliar pathogens infection. Later, Yoshioka et al. (2012) investigated that the mutation of *NPR1* impairing in NPR1 protein activity led to significant disease suppression lacking. As proline accumulation consideration, our result showed that proline was significantly accumulated in *T. harzianum*-treated seedlings with and without drought stress according to the *P5CS* gene expression. *P5CS* gene encodes to Δ'-pyrroline-5-carboxylate synthetase converting glutamatic acid to intermediate Δ'-pyrroline-5-carboxylate (P5C), then P5C is catalyzed by Δ'-pyrroline-5-carboxylate reductase (P5CR) to proline (Hayat et al., 2012.). The reciprocal regulation of *P5CS* and *proline dehydrogenase* (*PDH*) genes plays to be a key mechanism in the control of proline contents during and after osmotic stress (Peng et al., 1996). However, the researches involving effect of *T. harzianum* on *P5CS* expression have been found scarcely. Hence, we describe this event through the study of Choudhary et al. (2005) reported that *P5CS* expression was more in drought resistant rice than susceptible rice under drought subjection. Likewise, the study of Hong et al. (2000) investigated that feedback regulation of *P5CS* is lost in plants under osmotic stressed conditions. Then, we investigated effect of *T. harzianum* on *SPS1* expression under drought onset. *SPS1* gene encodes to sucrose phosphate synthase, a key regulatory enzyme in the pathway of sucrose biosynthesis. Several studies on important crops reported that *SPS* gene locus has been linked to control plant growth and yield (Kate Castleden et al., 2004). Our present result showed that *SPS1* expression was increased in treated plants under normal and stressed conditions. Correspondingly, Qazi and coworker (2014) indicated that *SPS* expression (*SPS1, 2, 3, 4* and *5*) was induced by drought stress in sorghum (*Sorghum bicolor* (L.) Moench). While, the present result exhibited that *SPS1* activity was slightly down regulated in uncolonized plant under drought stressed condition comparing to control plants. The study involving effect of *T. harzianum* on *SPS1* activation during drought stress was unclear. Liu et al. (2016) reported that *SPS* gene expression was increased in cabbage seedlings treating with chrysophanol, a secondary metabolite of *T. harzianum*, for 1 days under *Botrytis cinerea* infection for 3 day, whereas this gene expression was decreased in cabbage seedlings treating with *T. harzianum* for 3 day under the same condition. As different result, it may be due to the time period of treatment with *T. harzianum* was different. Accordingly, Shoresh et al. (2005) indicated that the expression of jasmonate/ethylene signaling pathways involved genes in cucumber preinoculating with *T. asperellum* were

increased at 24 and 48 h after challenging with *Pseudomonas syringae* pv. *lachrymans*, but were decreased below the control expression at 72 h after *P. syringae* challenge. The above results suggested that the timing for assessing the defense-related gene expression in a plant induced by *Trichoderma* colonization varies according to the plant-*Trichoderma* pathogen interaction.

Our results demonstrated that soil treating with *T. harzianum* can induce plant systemic resistance related gene which is *NPR1* and drought-responsive genes which are *P5CS* and *SPS1*. As above results, we conclude that *T. harzianum* can alleviate drought effect in rice seedlings through molecular alterations.

Acknowledgement

This work was supported by Science Achievement Scholarship of Thailand (SAST) and Salt-Tolerant Rice Research Group (STRG)

References

Bae, H., Sicher, R.C., Kim, M.S., Kim, S.H., Strem, M.D., Melnick, R.L., & Bailey, B.A. (2009). The beneficial endophyte *Trichoderma hamatum* isolate DIS 219b promotes growth and delays the onset of the drought response in *Theobroma cacao*. **Journal of Experimental Botany**. 60(11), 3279-3295.

Bassett, C.L., Baldo, A.M, Moore, J.T, Jenkins, R.M, Soffe, D.S, Wisniewski, M.E., … FarrellJr, R.E. (2014). Genes responding to water deficit in apple (*Malus × domestica* Borkh.) roots. **BioMed Central Plant Biology**. 14, 182-193.

Choudhary, N.L., Sairam, R.K., & Tyagi, A. (2005). Expression of *delta1-pyrroline-5-carboxylate synthetase* gene during drought in rice (*Oryza sativa* L.). ***Indian Journal of Biochemistry & Biophysics*.** 42(6), 366-370.

Hayat, S., Hayat, Q., Alyemeni, M.N., Wani, A.S., Pichtel, J., & Ahmad, A. (2012). Role of proline under changing environments. **Plant Signaling & Behavior**. 7(11), 1456-1466.

Hong, Z., Lakkineni, K., Zhang, Z., & Verma, D.P. (2000). Removal of feedback inhibition of delta(1)-pyrroline-5-carboxylate synthetase results in increased proline accumulation and protection of plants from osmotic stress. ***Plant Physiology*.** 122(4), 1129-1136.

Kate Castleden, C., Aoki, N., Gillespie, V.J., MacRae, E.A., Quick, W.P., Buchner, P., & Lunn, J.E. (2004). Evolution and function of the *Sucrose-Phosphate Synthase* gene families in wheat and other grasses. ***Plant Physiology***. 135(3), 1753-1764.

Liu, S.Y., Liao, C.K., Lo, C.T., Yang, H.H., Lin, K.C., & Peng, K.C. (2016). Chrysophanol is involved in the biofertilization and biocontrol activities of *Trichoderma*. ***Physiological and Molecular Plant Pathology*.** 96, 1-7.

Livak, K.J., & Schmittgen, T.D. (2001). Analysis of relative gene expression data using real-time quantitative PCR and the $2^{-\Delta\Delta CT}$ Method. ***Methods*.** 25(4), 402-408.

Ministry of Natural Resources and Environment. (2014). **Adaptation to drought affected areas.** Retrieved from http://www.environnet.in.th/?page_id=3760.

Nawrocka, J., & Małolepsza, U. (2013). Diversity in plant systemic resistance induced by *Trichoderma*. ***Biological Control***. 67(2), 149-156.

Okamura, M., Aoki, N., Hirose, T., Yonekura, M., Ohto, C., & Ohsugi, R. (2011). Tissue specificity and diurnal change in gene expression of the sucrose phosphate synthase gene family in rice. ***Plant Science***. 181(2), 159-166.

Peng, Z., Lu, Q., & Verma, D.P. (1996). Reciprocal regulation of *delta 1-pyrroline-5-carboxylate synthetase* and *proline dehydrogenase* genes controls proline levels during and after osmotic stress in plants. ***Molecular Genetics and Genomics***. 3, 334-341.

Qazi, H.A., Rao, P.S., Kashikar, A., Suprasanna, P., & Bhargava, S. (2014). Alterations in stem sugar content and metabolism in sorghum genotypes subjected to drought stress. **Functional Plant Biology.** 41, 954-962.

Salas-Marina, M.A., Silva-Flores, M.A. Uresti-Rivera, E.E., Castro-Longoria, E., Herrera-Estrella, A., & Casas-Flores, S. (2011). Colonization of *Arabidopsis* roots by *Trichoderma atroviride* promotes growth and enhances systemic disease resistance through jasmonic acid/ethylene and salicylic acid pathways. ***European Journal of Plant Pathology***. 131, 15-26.

Shoemaker, S., Schweikart, V., Ladner, M., Gelfand, D., Kwok, S., Myambo, K., & Innis, M. (1983). Molecular cloning of exo-cellubiohydrolase I derived from *Trichoderma reesei* strain L27. ***Nature Biotechnology***. 1, 691-696.

Shoresh, M., Yedidia, I., & Chet, I. (2005). Involvement of the jasmonic acid/ethylene signaling pathway in the systemic resistance induced in cucumber by *Trichoderma asperellum* T203. ***Phytopathology***. 95, 76-84.

Thai Rice Exporters Association. (2016). **Agricultural statistics of Thailand 2015.** Retrieved from http://www.oae.go.th/download/download_journal/2559/yearbook58.pdf.

Weindling R. (1932). *Trichoderma lignorum* as a parasite of other soil fungi. ***Phytopathology.*** 22, 837-845.

Wu, Y., Zhang, D., Chu, J.Y., Boyle, P., Wang, Y., Brindle, I.D, … Després, C. (2012). The *Arabidopsis* NPR1 protein is a receptor for the plant defense hormone salicylic acid. ***Cell Reports***. 1(6), 639-647.

Yoshioka, Y., Ichikawa, H., Naznin, H.A., Kogure, A., & Hyakumachi, M. (2012). Systemic resistance induced in *Arabidopsis thaliana* by *Trichoderma asperellum* SKT-1, a microbial pesticide of seedborne diseases of rice. ***Pest Management Science***. 68(1), 60-66.


มหาวิทยาลัยราชภัฏวไลยอลงกรณ์
VALAYA ALONGKORN RAJABHAT UNIVERSITY
ในพระบรมราชูปถัมภ์

ESTIMATION OF INTERFACE STATE DENSITY OF N-TYPE NANOCRYSTALLINE FESI2/P-TYPE SI HETEROJUNCTIONS IN MESA STRUCTURE FABRICATED BY UTILIZING PHOTOLITHOGRAPHY

Sakmongkon Teakchaicum[1], Peeradon Onsee[2], Asanlaya Duangrawa[3], Phongsaphak Sittimart[4], and Nathaporn Promros[5]

[1] affiliation curriculum bachelor's degree of science in applied physics faculty faculty of science university king mongkut's institute of technology ladkrabang email sakmongkon_teakchaicum@hotmail.com
[2] affiliation curriculum bachelor's degree of science in applied physics faculty faculty of science university king mongkut's institute of technology ladkrabang email peeradononsee@hotmail.com
[3] affiliation curriculum bachelor's degree of science in applied physics faculty faculty of science university king mongkut's institute of technology ladkrabang email asanlaya_duangrawa@hotmail.com
[4] affiliation curriculum master's degree of science in applied physics faculty faculty of science university king mongkut's institute of technology ladkrabang email psittimart@gmail.com
[5] affiliation curriculum doctoral degree of science in applied physics faculty faculty of science university king mongkut's institute of technology ladkrabang email nathaporn_promros@kyudai.jp

ABSTRACT

In the present study, n-type nanocrystalline (NC) $FeSi_2$/p-type Si heterojunctions in mesa structure were prepared by utilizing the lift-off photolithography method. The heterojunctions in mesa structure showed good rectifying behavior and response for the near-infrared light irradiation at room temperature. As compared to the n-type NC-$FeSi_2$/p-type Si heterojunctions in normal structure, the leakage current under reverse bias voltage condition was markedly reduced and the near-infrared light detection was clearly improved. In order to estimate the interface state density (N_{ss}) by using the Hill-Coleman method, the capacitance-voltage (*C-V*) and conductance-voltage (*G-V*) characteristics were measured in the applied frequency (*f*) value range from 50 kHz to 2 MHz, at room temperature. The N_{ss} values, which were reduced when compared with that of heterojunctions in normal structure, were 9.02×10^{13} $cm^{-2}eV^{-1}$ at 2 MHz and 1.26×10^{15} $cm^{-2}eV^{-1}$ at 50 kHz. The reduction of the N_{ss} value in the mesa structural heterojunctions was the main cause for the improvement of electrical properties at room temperature.

Keywords: Mesa Structural NC-$FeSi_2$/Si Heterojunction, Lift-off Photolithography, *IV* Characteristic, *C-V-f* Characteristic, *G-V-f* Characteristic

Introduction

Lately, the beta phase of semiconducting iron disilicide (β-$FeSi_2$), having component elements (Fe and Si) that are ecofriendly and abundant natural materials, has attracted much attention as a new promising candidate semiconductor for optoelectronic devices integrated with silicon (Leong et al., 1997; Promros et al., 2012). It has an optical absorption coefficient greater than 10^5 cm^{-1} at 1.2 eV, which is two orders of magnitude larger than that of Si (Promros et al., 2013). In addition, it possesses a direct optical band gap of 0.85 eV above an indirect optical band gap of 0.78 eV. These values of optical band gap correspond to the optical fiber telecommunication wavelengths of 1.31 and 1.55 μm (Promros et al., 2016). Nanocrystalline (NC) $FeSi_2$ is comprised of crystal with a diameter range of 3-5 nm and possesses semiconducting

features close to β-$FeSi_2$ (Promros et al., 2013). More importantly, it has a larger optical absorption coefficient than that of β-$FeSi_2$ (Takarabe et al., 2006) and can be grown on any solid substrate at room temperature (Promros et al., 2012). Thus, NC-$FeSi_2$ is also a new attractive material for optoelectronic applications.

Previously, the growth of NC-$FeSi_2$ films was achieved using pulsed laser deposition (PLD) (Yoshitake et al., 2003) and facing-target direct-current sputtering (FTDCS) (Shaban et al., 2008). n-Type NC-$FeSi_2$/p-type Si heterojunctions were fabricated and employed as photodiodes (Shaban et al., 2010). They exhibited large leakage current and weak response for near-infrared (NIR) light irradiation, which might be attributed to the interface states at the junction interfaces between the NC-$FeSi_2$ thin films and Si substrates. The existent interface states act as a leakage current center and trap center for photo-generated carriers and thus markedly degrade the NIR light detection performance (Funasaki et al., 2013; Promros et al., 2013; Promros et al., 2012). Subsequently, n-type NC-$FeSi_2$/p-type Si heterojunctions in mesa structures were fabricated by utilizing the lift-off photolithography method (Funasaki et al., 2013). The heterojunctions in mesa structure could reduce the junction capacitance and leakage current when compared to the heterojunctions in normal structure. Their near-infrared (NIR) light detection performance was improved at room temperature. This was possibly due to the interface states at the junction interface for heterojunction in mesa structure being reduced (Funasaki et al., 2013).

Research Objectives

In the present study, in order to estimate the density of the interface states (N_{ss}) based on the Hill-Coleman method, capacitance-voltage (*C-V*) and conductance-voltage (*G-V*) curves were measured and analyzed as a function of applied frequency (*f*). According to the estimation of the N_{ss} value from the obtained *C-V-f* and *G-V-f* curves, the N_{ss} value for the heterojunctions in mesa structure was reduced when compared with that of the pn heterojunctions in normal structure. For our beneficial knowledge, the present manuscript is the first investigation of the N_{ss} value at room temperature for n-type NC-$FeSi_2$/p-type Si heterojunctions in mesa structure.

Methodology

In order to remove the native oxide layer, a Si substrate was cleaned utilizing acetone, methanol, and distilled water for 5 minutes in sequence. After that, the Si substrate was dipped in dilute hydrofluoric (HF) acid solution, and then rinsed with deionized water. By utilizing a spin coating method, it was immediately coated with a resist liquid (ZPN-1150-90) for 30 seconds. The pattern was created by using ultraviolet light irradiation through a photo-mask for 13 seconds after pre-baking on a hot plate at 90 °C for 90 seconds. After post-baking on the hot plate at 110 °C for 70 seconds, the sample was dipped, for 60 seconds, in a developer (NMD-W 2.38 %). After that, it was rinsed with deionized water for 60 seconds. It was immediately set in FTDCS apparatus and then evacuated to a base pressure of 1×10^{-5} Pa using a turbo molecular pump. NC-$FeSi_2$ thin films with a thickness of 350 nm were formed onto the pattern at room temperature using $FeSi_2$ targets (purity: 4N). With a radio-frequency magnetron sputtering apparatus, Palladium (Pd) and Aluminium (Al) ohmic contacts were fabricated on the top of the Si substrates and on the bottom of the NC-$FeSi_2$ films,

respectively. Eventually, the resist was removed by immersion in a stripping solution for 15 minutes. The schematic of the heterojunctions in mesa structure is shown in Fig. 1.

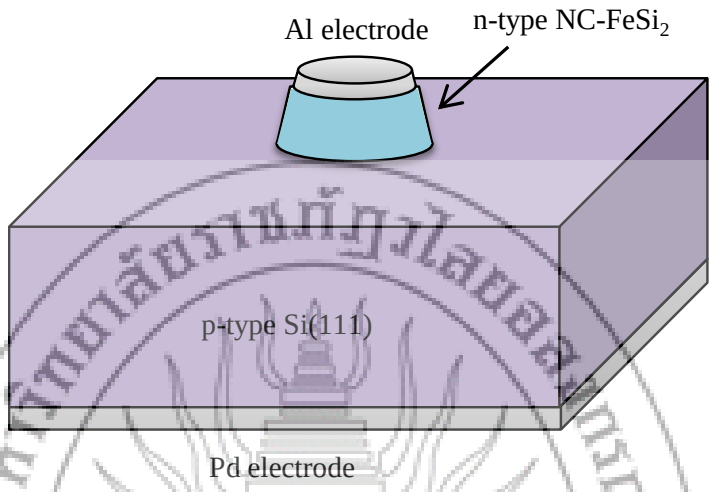

Figure 1. Schematic of n-type NC-$FeSi_2$/p-type Si heterojunctions in mesa structure.

By utilizing a source meter (Keithley 2400), the current density-voltage (*J-V*) curves of the mesa and normal structural heterojunctions were measured in the forward and reverse bias voltage conditions at room temperature, in the dark and under illumination of a 6 mW, 1.31μm laser (Neoark, TC20). By utilizing a precision LCR meter (Agilent, E4980A), the *C-V* and *G-V* curves at room temperature were measured as a function of the *f* value in the range from 50 kHz to 2 MHz in the dark. The N_{ss} value was calculated based on the Hill-Coleman method.

Research Results

Figure 2 presents the *J-V* curves of mesa structural heterojunctions at room temperature, in the dark and under illumination of a 6 mW, 1.31 μm laser diode and compared with those of the normal structural pn heterojunctions. The dark *J-V* curve for the normal structural pn heterojunctions exhibited rectifying action, which was similar to those of conventional pn heterojunctions. This action was accompanied by a large leakage current under reverse bias condition. In addition, the reverse current under illumination of the normal structural pn heterojunctions was extremely weak. In the case of the mesa structural pn heterojunctions, the *J-V* curve in the dark exhibited the improvement of rectifying action when compared with that of the normal structural pn heterojunctions. The reverse dark current for the mesa structural pn heterojunctions was decreased by more than one order of magnitude as compared with that of the normal structural pn heterojunctions. The ratio of the photocurrent to dark current for the mesa structural pn heterojunctions was clearly enhanced when compared with that of the normal structural pn heterojunctions. These results might be attributed to the reduction of interface states at the junction interface in the mesa structural pn heterojunctions (Funasaki et al., 2013; Promros et al., 2013; Promros et al., 2012).

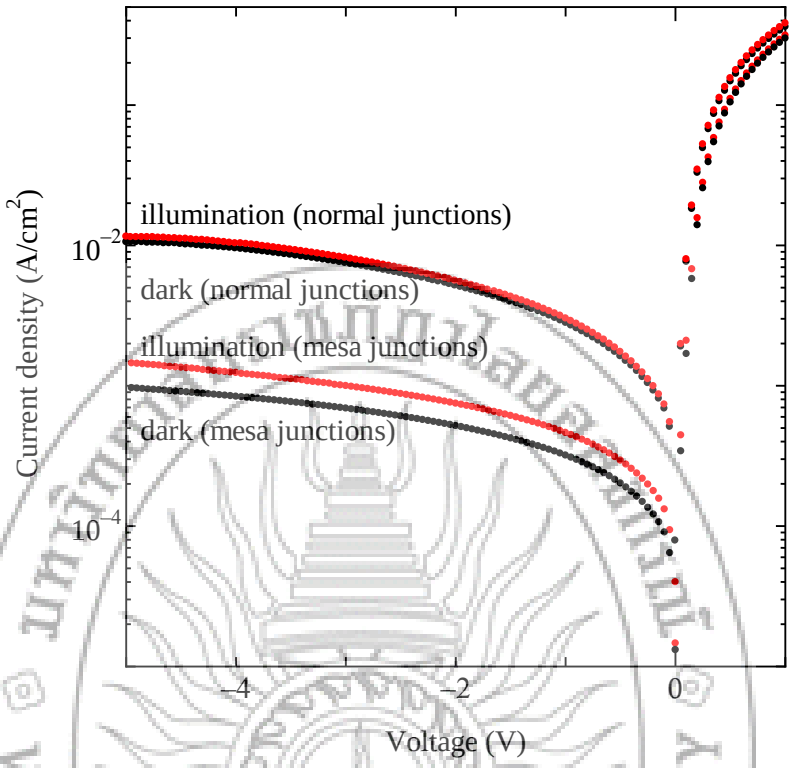

Figure 2. The *J-V* curves of mesa and normal structural n-type NC-$FeSi_2$/p-type Si heterojunctions in the dark and under illumination at room temperature under forward and reverse bias voltage conditions.

Figure 3 (a) presents the *C-V-f* curves of the heterojunctions in mesa structure. The measurements were carried out at an *f* value from 50 kHz to 2 MHz in the dark at room temperature. The *C* value decreased when the *f* value was increased. Figure 3 (b) displays the *G-V-f* characteristics for the heterojunctions in mesa structure. It was found that the *G* value increased with increasing *f* value.

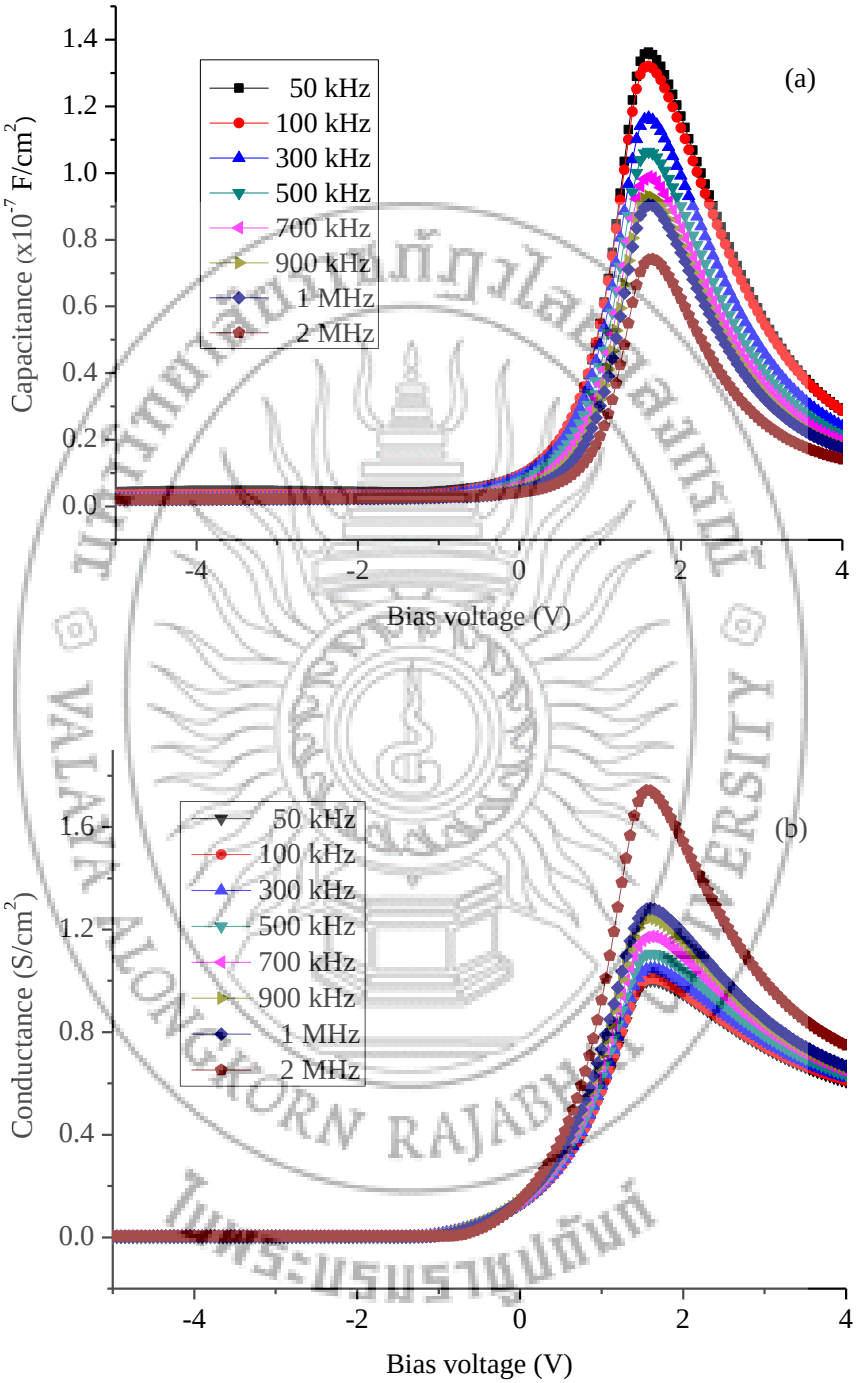

Figure 3. (a) *C-V-f* and (b) *G-V-f* curves of the heterojunctions in mesa structure at room temperature.

The value of N_{ss} is a vital factor for the electrical properties of the fabricated heterojunctions in mesa structure. The Hill-Coleman method is very appropriate for estimation of the N_{ss} value. Using this method, the N_{ss} value can be expressed as (Yahai et al., 2012; Ahmad et al., 2010):

$$N_{ss} = \frac{(G_m/\omega)_{max}}{((G_m/\omega)_{max}C_{ox})^2+(1-C_m/C_{ox})^2}\frac{2}{qA} \quad (1)$$

Here, ω is angular frequency, A is the area of the junction, C_m and $(G_m/\omega)_{max}$ are the measured capacitance and conductance, corresponding to the maximum values, and C_{ox} is the insulator oxide layer capacitance, which is expressed as:

$$C_{ox} = \left[1+\frac{G_m^2}{(\omega C_m)^2}\right]C_m \quad (2)$$

Figure 4 illustrates the plot of the N_{ss} value as a function of the f value for the pn heterojunctions in mesa structure and this plot was compared with that of pn heterojunctions in normal structure. The values of N_{ss} calculated by Eq. (1) were 9.02 x 10^{13} $cm^{-2}eV^{-1}$ at 2 MHz and 1.26 x 10^{15} $cm^{-2}eV^{-1}$ at 50 kHz. This result showed the existence of an interface state at the heterojunction interface. It likely acts as a leakage current center and a trap center for photo-generated carriers. However, the N_{ss} value of heterojunction in mesa structure was decreased as compared with the pn heterojunctions in normal structure. This result proved that interface states existed at the heterojunction interface, which acts as a trap center for the photo-generated carriers and leakage current center, were decreased in the mesa structural heterojunctions (Funasaki et al., 2013; Promros et al., 2013; Promros et al., 2012). This probably was the main reason for the reduction of leakage current density and the improvement in NIR light detection performance for the pn heterojunctions in mesa structure.

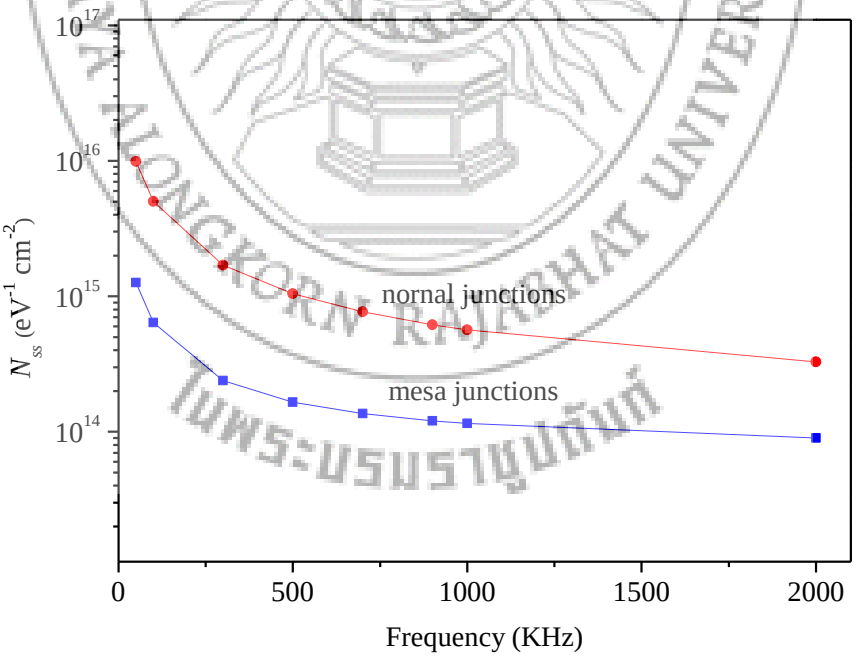

Figure 4. The plot of N_{ss}-f for the pn heterojunctions in mesa structure compared with the pn heterojunctions in normal structure.

Summary and Recommendation

In this research, n-type NC-$FeSi_2$/p-type Si heterojunctions in mesa structure were fabricated by means of lift-off photolithography. When compared to the n-type NC-$FeSi_2$/p-type Si heterojunction in normal structure, the leakage current under reverse bias voltage condition was markedly reduced and the NIR light detection was clearly improved. The N_{ss} values for the heterojunction in mesa structure were reduced when compared with those of heterojunction in normal structure, were 9.02×10^{13} $cm^{-2}eV^{-1}$ at 2 MHz and 1.26×10^{15} $cm^{-2}eV^{-1}$ at 50 kHz. This result confirms the improvement of the heterojunction interface for NC-$FeSi_2$/Si heterojunctions in mesa structure, which results in improved electrical properties in the fabricated heterojunctions.

Acknowledgement

This work was supported financially by a research fund from AUN/SEED-Net in the Collaborative Research Program for Alumni Members (CRA) Project and King Mongkut's Institute of Technology Ladkrabang.

References

Ahmad, Z., Sayyad, M. H., Karimov, Kh. S., Saleem, M., & Shah, M. (2010). Frequency dependent electrical characteristics of Au/*n*-Si/CuPc/Au heterojunction. **Acta Physica Polonica**. 117(3), 493-496.

Funasaki, S., Promros, N., Iwasaki, R., Takahara, M., Shaban, M., & Yoshitake, T. (2013). Fabrication of mesa structural n-type nanocrystalline-$FeSi_2$/p-type Si heterojunction photodiodes by liftoff technique combined with photolithography. **Status Solidi C Physica**. 10(12), 1785-1788.

Leong, D., Harry, M., Reeson, K. J., & Homewood, K. P. (1997). A silicon/iron-disilicide light-emitting diode operating at a wavelength of 1.5 μm. **Nature**. 387(6634), 686-688.

Promros, N., Baba, R., Takahara, M., Mostafa, T., Sittimart, P., Shaban, M., & Yoshitake, T. (2016). Epitaxial growth of β-$FeSi_2$ thin films on Si(111) substrates by radio frequency magnetron sputtering and their application to near-infrared photodetection. **Japanese Journal of Applied Physics**. 55(6S2), 06HC03-1-06HC03-4.

Promros, N., Chen, L., & Yoshitake, T. (2013). Near-infrared photodetection in *n*-type nanocrystalline $FeSi_2$/*p*-type Si heterojunctions. **Journal of Nanoscience and Nanotechnology**. 13(5), 3577-3581.

Promros, N., Yamashita, K., Iwasaki, R., & Yoshitake, T. (2012). Effects of hydrogen passivation on near-infrared photodetection of n-type β-$Fesi_2$/p-type Si heterojunction photodiodes. **Japanese Journal of Applied Physics**. 51(10R), 108006-1-108006-2.

Promros, N., Yamashita, K., Izumi, S., Iwasaki, R., Shaban, M., & Yoshitake, T. (2012). Near-infrared photodetection of n-type β-$Fesi_2$/intrinsic Si/p-type Si heterojunctions at low temperatures. **Japanese Journal of Applied Physics**. 51(9S2), 09MF02-1-09MF02-4.

Promros, N., Yamashita, K., Li, C., Kawai, K., Shaban, M., Okajima, T., & Yoshitake, T. (2012). n-Type nanocrystalline $FeSi_2$/intrinsic Si/p-type Si heterojunction photodiodes fabricated by facing-target direct-current sputtering. **Japanese Journal of Applied Physics**. 51(2R), 021301-1-021301-4.

Shaban, M., Kawai, K., Promros, N., & Yoshitake, T. (2010). n-Type nanocrystalline-$FeSi_2$/p-type Si heterojunction photodiodes prepared at room temperature. **IEEE Electron Device Letters**. 31(12), 1428-1430.Shaban, M.,

Kondo, H., Nakashima, K., & Yoshitake, T. (2008). Electrical and photovoltaic properties of n-type nanocrystalline-$FeSi_2$/p-type Si heterojunctions prepared by facing-targets direct-current sputtering at room temperature. **Japanese Journal of Applied Physics**. 47(7), 5420-5422.

Takarabe, K., Doi, H., Mori, Y., Fukui, K., Shim, Y., Yamamoto, N., Yoshitake, T., & Nagayama, K. (2006). Optical properties of nanocrystalline $FeSi_2$ and the effects of hydrogenation. **Applied Physics Letters**. 88(6), 061911-1-0619113.

Yahai, I. S., Fadel, M., Sakr, G. B., Shenouda, S. S., & Yakuphanoglu, F. (2012). Effect of the frequency and temperature on the complex impedance spectroscopy (*C-V* and *G-V*) of p-$ZnGa_2Se_4$/n-Si nanostructure heterojunction diode. **Journal of Materials Science**. 47(4), 1719-1728.

Yoshitake, T., Yatabe, M., Itakura, M., Kuwano, N., Tomokiyo, Y., & Nagayama, K. (2003). Semiconducting nanocrystalline iron disilicide thin films prepared by pulsed-laser ablation. **Applied Physics Letters**. 83(15), 3057-3059.

PREPARATION OF CHROMIUM ZINC PYROPHOSPHATE CATALYST FOR ALTERNATIVE ENERGY SYNTHESIS

Somsuk Trisupakitti[1]Sarin Thongthummachat[2]Butsayamat Rattanadon[3]and Pornpimol Ponkham[4]

[1-4] Department of Chemistry, Faculty of Science and Technology,
RajabhatMahasarakham University, Thailand
Email:somsuk_rmu@yahoo.com

ABSTRACT

The objective of this study was to examine the preparation process chromium zinc pyrophosphate ($CrZnP_2O_7$) catalyst for alternative energy synthesis for synthesis of dimethyl ether by using reactant substances such as chromium nitrate, zinc nitrate, and phosphoric acid under the process of co-precipitation method which then yielded the compound substances that included chromium hydrogen phosphate ($CrHPO_4{\cdot}0.75H_2O$) and zinc hydrogen phosphate ($ZnHPO_4{\cdot}0.75H_2O$). After that, those two compound substances were mixed using prescribed proportion of chromium hydrogen phosphate and zinc hydrogen phosphate ratio at 0:10 2:8 4:6 6:4 8:2 and 10:0. Then, they were analyzed for appropriate temperature in order to perform calcination. The Thermo Gravimetric Analysis (TGA) technique showed that the appropriate temperature was higher than 750 degree Celsius. After using Fourier Transform Infrared Spectroscopy (FT-IR) and X-ray Diffraction (XRD) techniques in verifying product identity undergone calcination, the results showed that there were 2 types of vibration of $P_2O_7^{4-}$ and H_2O molecules while the examination results from using XRD showed that crystallization and amorphousness of chromium zinc pyrophosphate rely one chromium and zinc ratio.

Keywords: chromium zinc pyrophosphate catalyst, alternative energy synthesis

Introduction

Today, the use of fuel energy in everyday life is at the very high level whether it is for transportation or electricity generation. This directly leads to the gradual reduction of nonrenewable fuel energy. Also, the price of fuel energy inevitably becomes more expensive and it has been predicted that fuel energy will be totally used up. So, human starts to develop alternative energy to use in place of nonrenewable fossil fuel without having an effect to the environment. Current options of renewable energy are, for example, biomass, wind, water, solar, and geothermal energy. These alternative energies highly gain public attention at the moment. Therefore, this research focuses on studying the use of synthesized gas from biomass to produce dimethyl ether.

Dimethyl Ether or DME has chemical formula as is ether-type oxygenate substance which holds gas condition without color at room temperature and pressure. The property of dimethyl ether is similar to liquid petroleum that has boiling point at -25 degree Celsius and vapor pressure at 6 bar at 25 degree Celsius so this gas is easily transformed into liquid using pressurization and it is popularly used in substitution of liquid petroleum without forming new basic foundation. When it is burnt and the burning is complete without generating soot. And, the release of carbon monoxide and oxide of nitrate is lower than other types of fuel energy. Also, it has no sulfur components so there is no sulfur dioxide that negatively affects the environment.

Moreover, it has high cetanenumber at 55-60 which can be used as alternative energy for diesel engine. Importantly, the gas does not provide harmful effects towards human and it can easily self-decomposed in the air.

The original production of methyl ether was indirect method by using the synthesized gas obtained from gasification of coal or biomass or reforming process of natural gas. They are mixed for reaction process to produce methanol. Then methanol will be dehydrated using acid reactor such as gamma alumina and zeolite within fixed-bed catalytic reactor at the temperature of 280 degree Celsius. Finally, the output is dimethyl ether and H_2O, but this method is pricy due to the cost of methanol as reactant is expensive. So, the current favorable production process is producing dimethyl ether directly from synthesized gas which has more advantages than the indirect method because that method does not involve synthesizing methanol which can reduce the production cost whereas this process involves taking synthesized gas to undergo heat process inside slurry reactor with using catalyst. This process in the industry uses zeolite but the cost of raw material producing zeolite is expensive and thus the price of zeolite.

So, this study pays attention to iron phosphate which is widely used in various activities such as fuel catalyst, magnetic device, ionic conductor. Phosphate catalyst can be synthesized by co-precipitation method which gives undissolved phosphate with crystalized structure or amorphousness. In addition, other synthesis methods could be used to serve this purpose such as hydrothermal, sol-gel process, and co-precipitation method. However, this study investigates the use of co-precipitation method of zinc pyrophosphate which has catalytic capacity similarly to that of zeolite but the preparation process is easier and thus the production cost is cheaper. Also, zinc pyrophosphate is a bifunctional catalyst so it is appropriate for synthesizing dimethyl ether from gas directly.

Research Objectives

The objective of this study was to examine the preparation process chromium zinc pyrophosphate ($CrZnP_2O_7$) catalyst for alternative energy synthesis for synthesis of dimethyl ether.

Methodology

1. Preparation of catalyst for chromium zinc pyrophosphate

(a)Preparation of hydrogen phosphate by co-precipitation method

Weigh 29.86 gram of chromium nitrate and 6.36 millilitres of phosphoric acid, mix into 250 millilitres of distilled water at room temperature, adjust pH at 8 by ammonia solution, shake for 24 hours, filter out sediments using pressure adjustable filter, wash sediments using distilled water until pH of solution equates to pH of distilled water, dehydrate for at 100 degree Celsius for 24 hours.

(b)Preparation of zinc hydrogen phosphate by co-precipitation method

The preparation process is similar to that done for chromium hydrogen phosphate but use only 25.52 grams of zinc nitrate and 5.87 millilitres of phosphoric acid.

(c)Preparation of chromium zinc pyrophosphate

Mix chromium hydrogen phosphate derived from process (a) with hydrogen phosphate gained from process (b) at the following mass ratio: 0:10 2:8 4:6 6:4 8:2

and 10:0. Take all proportions of solid items to undergo calcination at the temperature of 750 degree Celsius for 3 hours. Then, take sample substances for property verification.

2. Identity verification

The following techniques were used to verify the sample substances identity.

1. Examine heat behaviors by Thermo Gravimetric Analysis (TGA) in search for appropriate temperature for calcination.

2. Examine identity for basic substance vibration by Fourier Transform Infrared Spectroscopy (FT-IR) in search for categorical functions of substance.

3. Examine crystalization and amorphousness by X-ray diffractometer (XRD) in search for components of sample substance.

Research Results

1. Synthesis results of chromium zinc pyrophosphate by using co-precipitation method

The chromium zinc pyrophosphate synthesis process used $Cr(NO_3).6H_2O$ and $Zn(NO_3).6H_2O$ as reactants and H_3PO_4 as phosphate source by co-precipitation method that used 30% concentrated ammonia solution to control pH at 8 which is the most workable value that can generate chromium hydrogen phosphate and zinc. And, they could be brought to synthesize for zinc pyrophosphate by mixing these two substances and undergoing calcination. The reaction can be outlined as 1-3 equations. And, from Table 1, it was found that $CrZnP_2O_7$ at the Cr:Zn ratio of 8:2 provided the highest yield at 92.66% while $Cr_2P_2O_7$ provided the lowest yield at 78.76%.

$$Cr(II)(NO_3)_2.9H_2O(s) + H_3PO_4 \rightarrow Cr(II)HPO_4{\cdot}0.75H_2O(s) + 2NO_3^- + 2H^+ + 8.25H_2O \quad (1)$$

$$Zn(II)(NO_3)_2.6H_2O(s) + H_3PO_4 \rightarrow Zn(II)HPO_4{\cdot}0.75H_2O(s) + 2NO_3^- + 2H^+ + 5.25H_2O \quad (2)$$

$$Zn(II)HPO_4.0.75H_2O(s) + Cr(II)HPO_4.0.75H_2O(s) \rightarrow CrZnP_2O_7(s) + 2.5H_2O \quad (3)$$

Table 1. Production percentage of chromium zinc pyrophosphate synthesized by co-precipitation method

Products	Substance Weight (gram)	Yield (%)
$Cr_2P_2O_7$	6.3008	78.76
$CrZnP_2O_7$ Cr:Zn ratio at 2:8	6.3392	79.24
$CrZnP_2O_7$ Cr:Zn ratio at 4:6	6.5880	82.35
$CrZnP_2O_7$ Cr:Zn ratio at 6:4	6.7456	84.32
Products	Substance Weight (gram)	Yield (%)
$CrZnP_2O_7$ Cr:Zn ratio at 8:2	7.4128	92.66
$Zn_2P_2O_7$	7.2144	90.18

2. Decomposition using heat by TGA technique

Examination of heat behavior used Thermo Gravimetric Analysis (TGA), Perkin, Pyris 1 model. This technique could identify heat stability and the thermogram data could be used to determine combustion range of $Zn(II)HPO_4{\cdot}0.75H_2O$ and $Cr(II)HPO_4{\cdot}0.75H_2O$ which conform to 3 ranges dehydration: 1) at the temperature of 50-90 degree Celsius in which the dehydration occurs inside the crystal; 2) at the temperature of 90-200 degree Celsius which might be the result of dehydration of $Zn(II)HPO_4{\cdot}0.75H_2O$ and $Cr(II)HPO_4{\cdot}0.75H_2O$; and 3) at the temperature of 200-750 degree Celsius which might result from the evolvement of $Cr_2P_2O_7$ and $Zn_2P_2O_7$ from reaction 4-5 equations and the output shown in Figure 1-2.

$$2Cr(II)HPO_4{\cdot}0.75H_2O(s) \rightarrow Cr2P_2O_7(s) + 1.75H_2O \quad (4)$$

$$2Zn(II)HPO_4{\cdot}0.75H_2O(s) \rightarrow Zn2P_2O_7(s) + 1.75H_2O \quad (5)$$

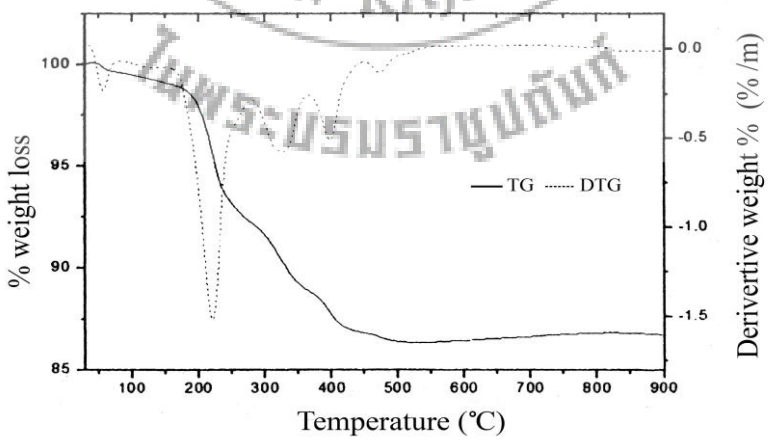

Figure 1. TG and DTG curves of $ZnHPO_4$ prepared from $Zn(NO_3)_2$ and H_3PO_4

Thermogram analysis results in Figure 1 indicated the weight loss at temperature of 40-90 degree Celsius accounting for 0.677% which resulted from moisture release of hydro in the crystal. At the temperature of 90-200 degree Celsius revealed the loss of weight accounting for 7.084% which resulted from dehydration of $Zn(II)HPO_4 \cdot 0.75H_2O$. At the temperature of 200-550 degree Celsius showed the loss of weight accounting for 5.408% which resulted from evolvement of $Zn_2P_2O_7$ whereas zinc hydrogen phosphate were transformed into amorporus-pyrophosphate at the temperature of 300-550 degree Celsius. At the temperature of 400-500 degree Celsius, revealed the two-tier of weight loss were which resulted in evolvement of $Zn_3(PO_4)_2$ and $Zn_2P_2O_7$ crystallization.

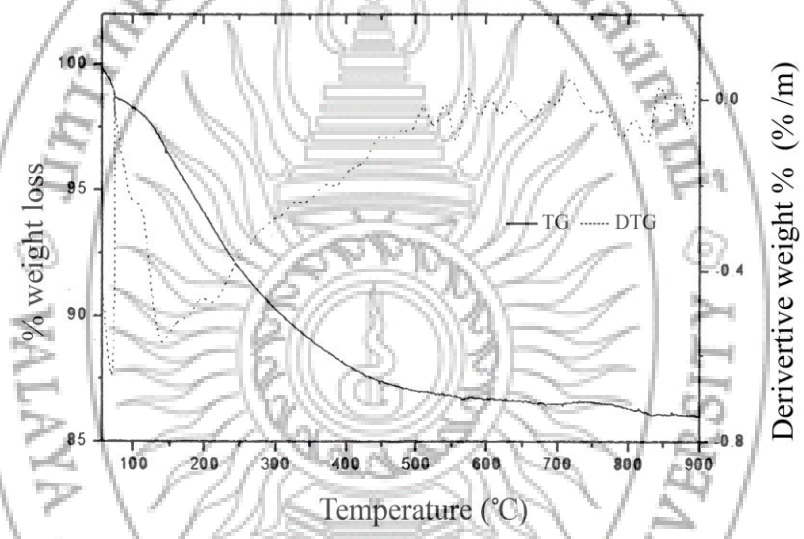

Figure 2. TG and DTG curves of $CrHPO_4$ prepared from $Cr(NO_3)_2$ and H_3PO_4

Thermogram analysis results in Figure 2 indicated the weight loss at the temperature of 50-70 degree Celsius accounting for 1.31% of weight loss due to moisture release of water in the crystal. At the temperature of 70-300 degree Celsius revealed the weight loss at 0.86% due to dehydration of $Cr(II)HPO_4 \cdot 0.75H_2O$. At the temperature of 300-750 degree Celsius revealed the weight loss at 11.05% which resulted in evolvement of $Cr_2P_2O_7$.

3. Identity verification of basic substance vibration by using FT-IR technique

The spectra records of FT-IR as shown in Figure 3-7 by categorizing vibration patterns were substances under hydrogen phosphate category which consists of 2 vibration patterns including HPO_4^{2-} and water molecules. The basic vibration pattern of HPO_4^{2-} indicated unique vibration pattern at the position of 350-580, 700-900, 860-915, 940-1010, 1040-1170, 1210-1400, 2600-3250 cm^{-1} or it could be called vibration pattern O_3-P-O bending, P-O-H stretching, P-O(H) stretching, $\nu_s(PO_3)$,$\nu_{as}(PO_3)$, P-O-H bending and ν(OH) respectively. Vibration pattern ν(OH) showed vibration at the

range of 600-1700, 3100-3146, 3200-3400 cm^{-1} which could be called vibration pattern $\nu_s(POP)$, $\nu_s(PO_2)$, and $\nu_{as}(PO_2)$ respectively.

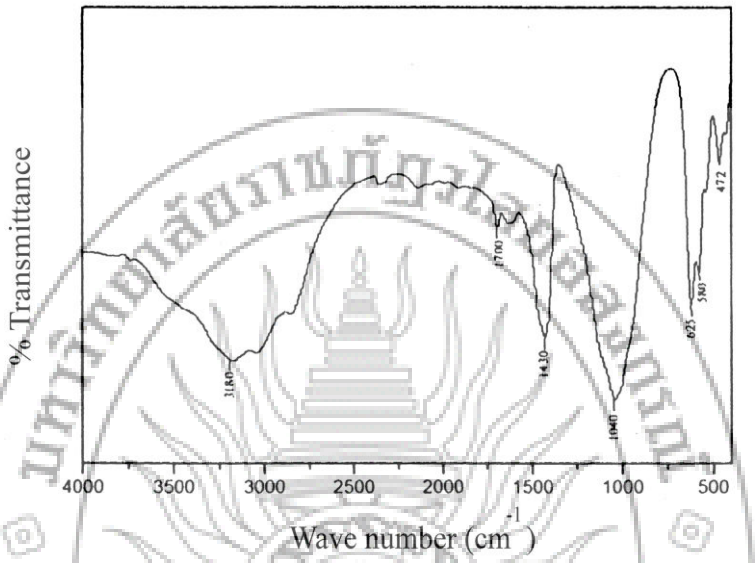

Figure 3. FT-IR spectra of $Zn(II)HPO_4{\cdot}0.75H_2O$ prepared by co-precipitation method of $Zn(II)(NO_3)_2{\cdot}6H_2O$ and H_3PO_4 which adjusted pH at 8

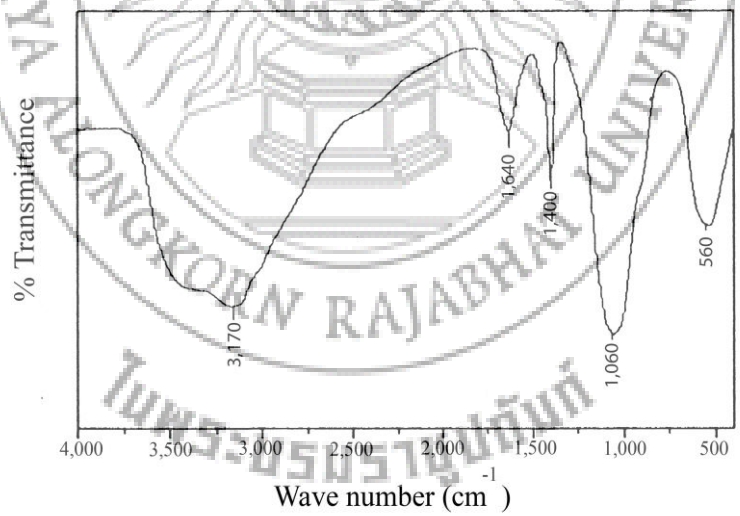

Figure 4. FT-IR spectra of $Cr(II)HPO_4{\cdot}0.75H_2O$ prepared by co-precipitation method of $Cr(II)(NO_3)_2{\cdot}9H_2O$ and H_3PO_4 which adjusted pH at 8

According to Figure 3-4, it was found that substance undergone synthesizing showed vibration spectrum of hydrogen phosphate $(HPO_4)^{2-}$ and water molecules which conform to basic vibration pattern as outlined above. This meant that the synthesized substance could be hydrogen phosphate.

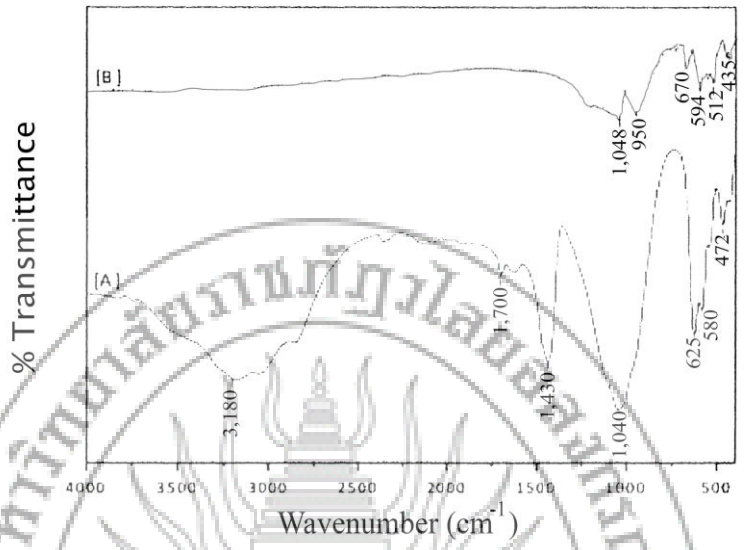

Figure 5. FT-IR spectra of substance [A] $Zn(II)HPO_4 \cdot 0.75H_2O$ by comparison with [B] $Zn_2P_2O_7$ obtained from calcination $ZnHPO_4 \cdot 0.75H_2O$at 750 degree Celsius

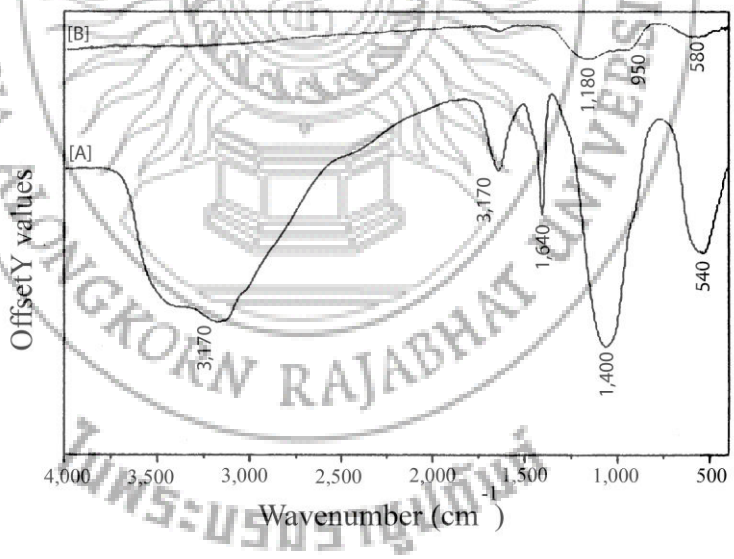

Figure 6 FT-IR spectra of substance [A] $Cr(II)HPO_4 \cdot 0.75H_2O$ by comparison with [B] $Cr_2P_2O_7$ obtained from calcination $CrHPO_4 \cdot 0.75H_2O$ at 750 degree Celsius

According to Figure 5-6, it was found that synthesized substance [B] showed vibration spectrum of pyrophosphate$(P_2O_7)^{4-}$ which conform to the basic vibration pattern as outlined above.

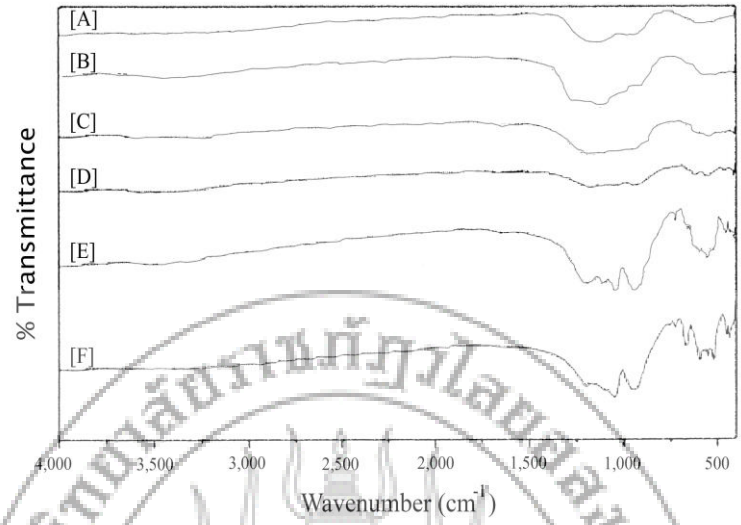

Figure 7 FT-IR spectra of substance $CrZnP_2O_7$ derived from calcinations $CrHPO_4{\cdot}0.75H_2O$and $ZnHPO_4{\cdot}0.75H_2O$ at 750 degree Celsius at different ratio

[A] $CrZnP_2O_7$ at Cr:Zn ratio was 10:0 [B] $CrZnP_2O_7$ at Cr:Zn ratio was 2:8
[C] $CrZnP_2O_7$ at Cr:Zn ratio was 4:6 [D] $CrZnP_2O_7$ at Cr:Zn ratio was 6:4
[E] $CrZnP_2O_7$ at Cr:Zn ratio was 8:2 [F] $CrZnP_2O_7$ at Cr:Zn ratio was 0:10

According to Figure 7, it was found that the synthesized substance showed vibration spectrum of pyrophosphate $(P_2O_7)^{4-}$ and the vibration of pyrophosphate $(PO_4)^{3-}$ conform to the basic vibration pattern as outlined above which meant that the synthesized substances might be pyrophosphate.

4. Analysis of crystallisation and amorphousness by using XRD technique

XRD is a technique relying on diffraction and scattering of of x-ray within the material by using Bruker AXS X-ray diffraction analysis equipment, D8 advance model. The synthesized substance is brought to analyze the structure against the standard graph in order to confirm that the synthesized substance has crystallisation property similarly to that that of $Cr_2P_2O_7$, $Zn_2P_2O_7$ and $CrZnP_2O_7$ as shown in Figure 8-10.

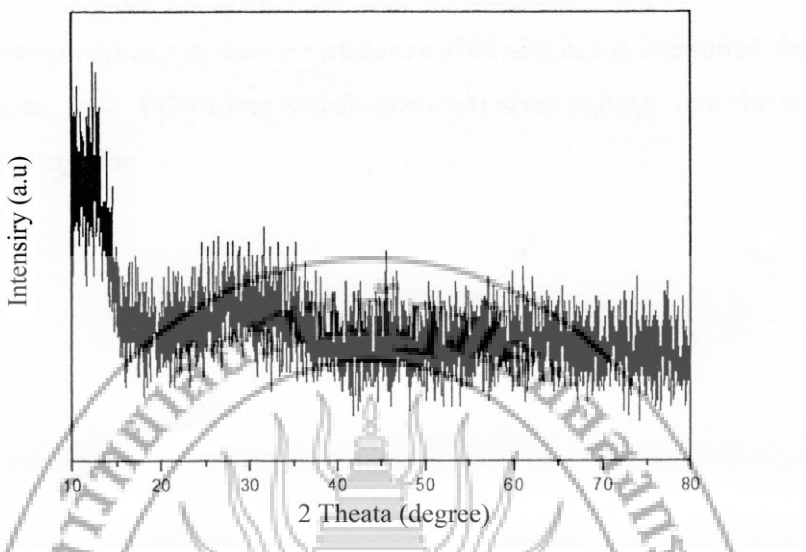

Figure 8 X-ray diffraction patterns of $Cr_2P_2O_7$

According to Figure 8, it was found that XRD graph of $Cr_2P_2O_7$ indicated high degree of amorphousness and it was unable to calculate for crystallization property which meant that the synthesized substance was not $Cr_2P_2O_7$.

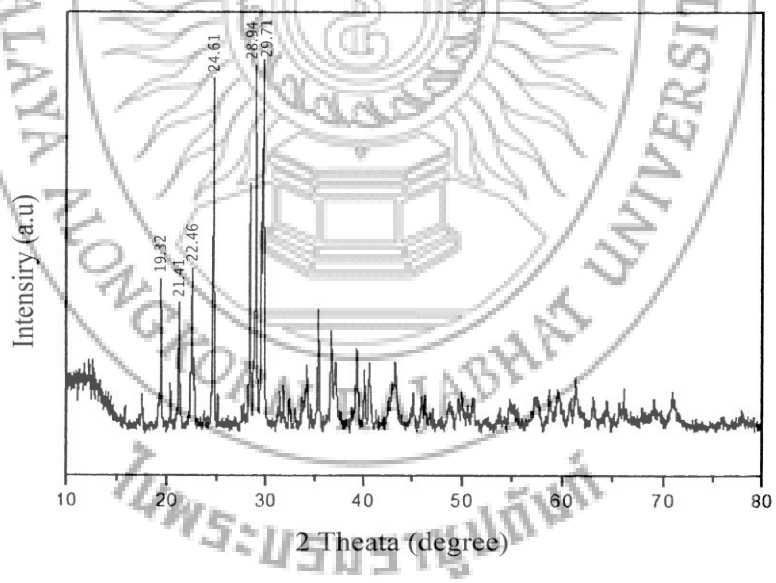

Figure 9 X-ray diffraction patterns of $Zn_2P_2O_7$

According to Figure 9, it was found that XRD graph of $Zn_2P_2O_7$ indicated the influential peak at 29.71. This value conformed to the standard graph of $Zn_2P_2O_7$ which meant that the synthesized substance was $Zn_2P_2O_7$. Also, the influential peaks were found at 19.32, 21.14, 22.46, and 24.61 which indicated standard value of standard graph of $Zn_3(PO_4)_2$ which meant that $Zn_3(PO_4)_2$ was also the product of the synthesis.

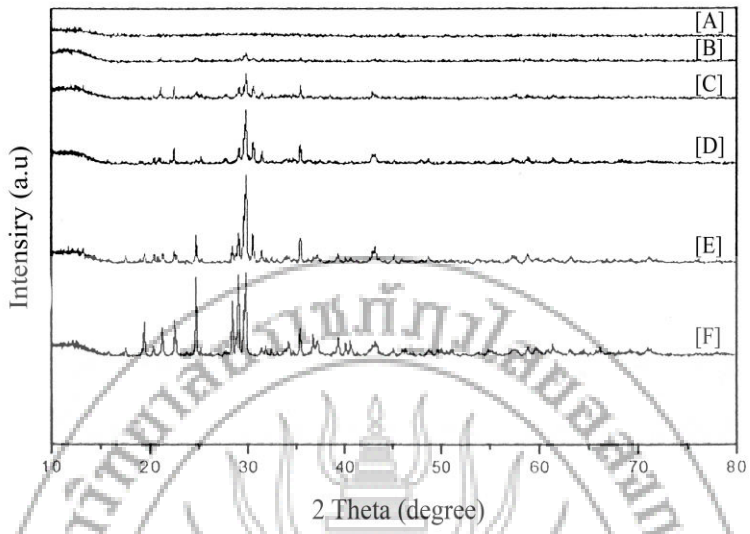

Figure 10 X-ray diffraction patterns of sample with comparison of different ratio
[A] $CrZnP_2O_7$ at Cr:Zn ratio was 10:0 [B] $CrZnP_2O_7$ at Cr:Zn ratio was 2:8
[C] $CrZnP_2O_7$ at Cr:Zn ratio was 4:6 [D] $CrZnP_2O_7$ at Cr:Zn ratio was 6:4
[E] $CrZnP_2O_7$ at Cr:Zn ratio was 8:2 [F] $CrZnP_2O_7$ at Cr:Zn ratio was 0:10

According to Figure 10, it was found that the ratio of high Zn but low Cr tended to evolve high degree of crystallisation. But, when the ratio was low Zn but high Cr, it tended to evolve amorphousness. Taken the output to calculate lattice parameter and size of crystallization, it was found that $Cr_2P_2O_7$ had high degree of amorphousness so it could not be used to calculate for crystallization. But, calculation crystallization of $Zn_2P_2O_7$ was at 85.52 nm while $CrZnP_2O_7$ had no standard graph for comparison so what could have been done was prediction on its crystallization size.

Summary and Recommendation

Synthesis of $CrZnP_2O_7$ could be done by using $Cr(NO_3)_2$ and $Zn(NO_3)_2$ as reactants and H_3PO_4 as phosphate source. It was found that the production percentages were 78.76, 92.66, 84.32, 82.35, 79.24, and 90.18 whereas the mass ratio of $CrHPO_4$ and $ZnHPO_4$ was at 10:0, 8:2, 6:4, 4:6, 8:2, 0:10 respectively.Identity verification of $Zn_2P_2O_7$ indicated that the synthesized substances were $ZnHPO_4$ and $Zn_2P_2O_7$ which contained high degree of crystallization and the size of crystallization was 82.52 nm.Identity verification of $Cr_2P_2O_7$ was unable to synthesize by using co-precipitation method. The FT-IR results were unable to clearly confirm that the synthesized substances were $ZnHPO_4$ and $Zn_2P_2O_7$. The XRD results indicated that the synthesized substances holding high degree of amorphousness were unable to calculate the size of crystallization.

Identity verification of $CrZnP_2O_7$ was unable to synthesize by using co-precipitation method. The FT-IR results were unable to clearly confirm that the synthesized substance was $CrZnP_2O_7$. The XRD results indicated that the synthesized substance holding either high crystallisation or amorphousness depended on the amount of Cr and Zn within its structure. Therefore, the substance holding high ratio of Zn

would contain high degree of crystallization, but the XRD results revealed high degree of amorphousness so it was unable to calculate the size of crystallization.

Acknowledgement

The authors desire to thank the Department of Chemistry of King Mongkut's Institute of Technology Ladkrabang for detecting the TGA, FT-IR and XRD.

References

Ali Hadipour & Morteza Sohrabi. (2008). Synthesis of some bifunctional catalysts and determination of kinetic parameters for direct conversion of syngas to dimethyl ether. **Chemical Engineering Journal**. 137, 294-301.

Banjong Boonchom & Nart Phuvongpha. (2009). Synthesis of new binary cobalt iron pyrophosphate ($CoFeP_2O_7$). **Journal of Materials Letters**. 63, 1709-1711.

Dingfeng Jin, Bing Zhu, Zhaoyin Hou, Jinhua Fei, Hui Lou & Xiaoming Zheng. (2007). Dimethyl ether synthesis via methanol and syngas over rare earth metals modified zeolite Y and dual Cu-Mn-Zn catalysts. **Journal of Fuel**. 86, 2707-2713.

Heqing Jiang, Hans Bongard, Wolfgang Schmidt & Ferdi Schuth. (2012). One-pot synthesis of mesoporous Cu-γ-Al_2O_3 as bifunction catalyst for direct dimethyl ether synthesis. **Journal of Microporous and Mesoporous Materials**. 164, 3-8.

Miriam Stiefel, Ruaa Ahmad, Ulrich Arnold & Manfred Doring. (2011). Direct synthesis of dimethyl ether from carbon-monoxide-rich synthesis gas: Influence of dehydration catalysts and operating conditions. **Journal of Fuel Processing Technology**. 92, 1466-1474.